(2)

POR-2033(EX)
(WT-2033)(EX)
EXTRACTED VERSION

OPERATION DOMINIC

CHRISTMAS AND FISH BOWL SERIES

PROJECT OFFICERS REPORT — PROJECT 7.1

ELECTROMAGNETIC SIGNAL, UNDERWATER MEASUREMENTS

A.P. Bridges, Project Officer
B.J. Bittner
V.D. Peckham
A.D. Moorhead
E.L. Cole
S.A. Bliss

Kaman Nuclear
Colorado Springs, Colorado

NOTICE:
This is an extract of POR-2033 (WT-2033), Operation DOMINIC, Christmas and Fish Bowl Series, Project Officers Report, Project 7.1.

Approved for public release;
distribution is unlimited.

Extracted version prepared for
Director
DEFENSE NUCLEAR AGENCY
Washington, DC 20305-1000

1 April 1985

38

Destroy this report when it is no longer needed. Do not return to sender.

PLEASE NOTIFY THE DEFENSE NUCLEAR AGENCY, ATTN: STTI, WASHINGTON, DC 20305-1000, IF YOUR ADDRESS IS INCORRECT, IF YOU WISH IT DELETED FROM THE DISTRIBUTION LIST, OR IF THE ADDRESSEE IS NO LONGER EMPLOYED BY YOUR ORGANIZATION.

UNCLASSIFIED
SECURITY CLASSIFICATION OF THIS PAGE

AD-A995288

REPORT DOCUMENTATION PAGE

Form Approved
OMB No. 0704-0188
Exp. Date: Jun 30, 1986

1a. REPORT SECURITY CLASSIFICATION UNCLASSIFIED	1b. RESTRICTIVE MARKINGS
2a. SECURITY CLASSIFICATION AUTHORITY	3. DISTRIBUTION/AVAILABILITY OF REPORT Approved for public release; distribution is unlimited.
2b. DECLASSIFICATION/DOWNGRADING SCHEDULE	
4. PERFORMING ORGANIZATION REPORT NUMBER(S)	5. MONITORING ORGANIZATION REPORT NUMBER(S) POR-2033(EX) (WT-2033(EX))
6a. NAME OF PERFORMING ORGANIZATION Kaman Nuclear 6b. OFFICE SYMBOL (If applicable)	7a. NAME OF MONITORING ORGANIZATION Defense Atomic Support Agency
6c. ADDRESS (City, State, and ZIP Code) Colorado Springs, CO	7b. ADDRESS (City, State, and ZIP Code) Washington, DC
8a. NAME OF FUNDING/SPONSORING ORGANIZATION 8b. OFFICE SYMBOL (If applicable)	9. PROCUREMENT INSTRUMENT IDENTIFICATION NUMBER
8c. ADDRESS (City, State, and ZIP Code)	10. SOURCE OF FUNDING NUMBERS PROGRAM ELEMENT NO. / PROJECT NO / TASK NO. / WORK UNIT ACCESSION NO.

11. TITLE (Include Security Classification)
OPERATION DOMINIC, CHRISTMAS AND FISH BOWL SERIES, PROJECT OFFICERS REPORT - PROJECT 7.1, ELECTROMAGNETIC SIGNAL, UNDERWATER MEASUREMENTS, EXTRACTED VERSION

12. PERSONAL AUTHOR(S)
A.P. Bridges, B.J. Bittner, V.D. Peckham, A.D. Moorhead, E.L. Cole, and S.A. Bliss

13a. TYPE OF REPORT	13b. TIME COVERED	14. DATE OF REPORT (Year, Month, Day)	15. PAGE COUNT
	FROM _____ TO _____	Undated [19637	97

16. SUPPLEMENTARY NOTATION This report has had sensitive military information removed in order to provide an unclassified version for unlimited distribution. The work was performed by the Defense Nuclear Agency in support of the DoD Nuclear Test Personnel Review Program.

17. COSATI CODES		
FIELD	GROUP	SUB-GROUP
18	3	
20	14	

18. SUBJECT TERMS (Continue on reverse if necessary and identify by block number)
Dominic
Underwater Detection
Electromagnetic Signals
Electromagnetic Detection

19. ABSTRACT (Continue on reverse if necessary and identify by block number)
This project was conducted to obtain measurements of the electromagnetic (EM) signals from nuclear detonations at large distances from the detonation point, above and beneath the sea surface. The planned use of the data is that of determining the feasibility of an Indirect Bomb Damage Assessment (IBDA) systemn based on the nuclear EM signature. The specific tests were conducted from two ships.

The EM signatures recorded both above and below the water surface for the various nuclear events are unique, recognizable, and predictable to a useful degree. It appears entirely feasible to utilize this nuclear EM signal as a method of IBDA.

The significance of the data presented herein lies primarily in the demonstrated ability to detect an above-water EM signal with an underwater antenna system. Signal characteristics are changed in magnitude and phase but are very easily recognizable with but a minimum of measuring equipment.

20. DISTRIBUTION/AVAILABILITY OF ABSTRACT	21. ABSTRACT SECURITY CLASSIFICATION
☒ UNCLASSIFIED/UNLIMITED ☐ SAME AS RPT. ☐ DTIC USERS	UNCLASSIFIED
22a. NAME OF RESPONSIBLE INDIVIDUAL Betty L. Fox	22b. TELEPHONE (Include Area Code) 202-325-7042 / 22c. OFFICE SYMBOL STTI

DD FORM 1473, 84 MAR 83 APR edition may be used until exhausted. All other editions are obsolete.

SECURITY CLASSIFICATION OF THIS PAGE
UNCLASSIFIED

19. ABSTRACT (Continued)

Reliability of the data taken on film records is considered to be good because of the instrumentation and calibrations used. The initial portion of the signal was lost on the majority of the signals due to triggering difficulties, but the maximum amplitude and phase relationships were recorded.

FOREWORD

Classified material has been removed in order to make the information available on an unclassified, open publication basis, to any interested parties. The effort to declassify this report has been accomplished specifically to support the Department of Defense Nuclear Test Personnel Review (NTPR) Program. The objective is to facilitate studies of the low levels of radiation received by some individuals during the atmospheric nuclear test program by making as much information as possible available to all interested parties.

The material which has been deleted is either currently classified as Restricted Data or Formerly Restricted Data under the provisions of the Atomic Energy Act of 1954 (as amended), or is National Security Information, or has been determined to be critical military information which could reveal system or equipment vulnerabilities and is, therefore, not appropriate for open publication.

The Defense Nuclear Agency (DNA) believes that though all classified material has been deleted, the report accurately portrays the contents of the original. DNA also believes that the deleted material is of little or no significance to studies into the amounts, or types, of radiation received by any individuals during the atmospheric nuclear test program.

ABSTRACT

Kaman Nuclear conducted tests under Project 7.1 with the objective of obtaining measurements of the electromagnetic (EM) signals from nuclear detonations at large distances from the detonation point, above and beneath the sea surface. The planned use of the data is that of determining the feasibility of an Indirect Bomb Damage Assessment (IBDA) system based on the nuclear EM signature.

The tests completed under Project 7.1 have provided experimental data useful to the above requirements. One of the primary tasks accomplished was a determination of the actual distortion of the EM transient signal as it propagates down through sea water. This is important because the sea water has a conductivity and phase shift that is frequency dependent for VLF signals. The resulting data demonstrates this distortion of the highly complex EM signal and will help define the limits and desirable specifications for a practical, operational, Polaris-EM-IBDA system.

The specific tests were conducted from two ships. One ship had a calibrated, above-water, whip antenna plus an underwater long wire (standard submarine type) antenna. The other ship had an identical installation, except that the underwater antenna was a 6- by 6-foot loop antenna set at various depths. Broadband video outputs from these four antennas were presented on scopes and photographed and recorded on magnetic tape.

The EM signatures recorded both above and below the water surface for the various nuclear events are unique, recognizable, and predictable to a useful degree. It appears entirely feasible to utilize this nuclear EM signal as a method of IBDA.

The significance of the data presented herein lies primarily in the demonstrated ability to detect an above-water EM signal with an underwater antenna system. Signal characteristics are changed in magnitude and phase but are very easily recognizable with but a minimum of measuring equipment.

Reliability of the data taken on film records is considered to be good because of the instrumentation and calibrations used. The initial portion of the signal was lost on the majority of the signals due to triggering difficulties, but the maximum amplitude and phase relationships were recorded.

PREFACE

This investigation was initiated and funded by the Special Projects Office, Mr. D. R. Williams, SP-2721, Department of the Navy, Washington 25, D. C., as Contract NOrd 18098(FBM) to Kaman Nuclear, Colorado Springs, Colorado. Project Number 7.1 was assigned by the Defense Atomic Support Agency, Washington 25, D. C.

An essential part of the instrumentation, installation, and operational arrangements were handled by Mr. Harvey Meeker, Technical Director, Mr. Senyu Ueunten, Mr. Al Chang, and other members of the Quality Evaluation Laboratory, Naval Ammunition Depot, Oahu, Hawaii.

Considerable assistance in the technical planning also was supplied by:

D. R. Williams, SP-2721, Special Projects Office
A. G. Jean, NBS, Boulder, Colorado
R. K. Moore, KU, Lawrence, Kansas
CAPT V. J. Veasey, USN, Special Projects Office
S. Fratianni, NRL, Washington, D. C. and
Dr. Ralph Partridge, University of Hawaii (now at Los Alamos Scientific Laboratory

The men and officers of the USS INFLICT and the USS LOYALTY and Commanding Officers CDR Denny and LCDR Taylor are commended particularly for their demonstration of U. S. Navy professional skill and willing dedication.

CONTENTS

CHAPTER 1

INTRODUCTION

The electromagnetic (EM) signal from a nuclear detonation has a waveform that has definite characteristics and is repeatable. It has been proposed to use this phenomena as the basis of a terminal surveillance system for use aboard the Polaris submarines. Actual measurements of the air-water transitional effects upon these signals are thus desirable.

1.1 OBJECTIVES

This project obtained measurements of the electromagnetic signals from nuclear detonations at large distances (offshore from Hawaii) from the detonation point, above and beneath the sea surface in order to determine the feasibility of utilizing the nuclear EM signature as a method of Indirect Bomb Damage Assessment (IBDA). These typically large distances result in a received signal combining both the direct and multiple-bounce reflected components, which is the case for all typical Polaris missile trajectories. Generally, close-in and greater range capabilities of the system will be assessed by comparison and extrapolation from records of the signal made

by other projects at these ranges. These measurements are to provide data on the effect of the air-water phase shift and attenuation on transmission of the very low frequency (VLF) electromagnetic signals from near-surface and high-altitude bursts.

1.2 BACKGROUND

Present data (Reference 1) indicates that it is possible to use the EM signal from a nuclear detonation for a Terminal Surveillance System or IBDA, as the time of the event is a predictable, direct function of range to target. It is desired to use present VLF submarine communications antennas for this purpose; therefore, knowledge of the effect of the air-water mode conversion of the signal and subsequent attenuation by water of the EM signal is necessary for proper operation.

Data from U.S. (and other) nuclear tests and recorded background spherics indicate the feasibility of using the EM signals from a Polaris warhead for IBDA at distances applicable to IRBM ranges. The submarine commander would thereby be provided with a means of determining warhead functioning at the target, with a subsequent savings of missiles and/or added confidence of target kill and/or an extension of target damage for the number of missiles.

No known underwater measurements of the VLF EM signal from a nuclear detonation have been made to date. Additional background details may be obtained from References 2 and 3.

1.3 THEORY

1.3.1 Generation of EM Field. The phenomenon on which the Terminal Surveillance System is based is the receipt of the VLF transient electromagnetic signal from the burst. In order to describe the behavior of the pulse as a function of yield and distance, it is necessary to state the principal causes of the signals and the propagation characteristics.

While the mechanism for the generation of the electromagnetic signal is not understood in detail, certain theories have gained general acceptance (References 4 and 5). These theories indicate that a complex set of mechanisms is involved. Basically, the EM signal is believed to result initially from the creation and motion of Compton electrons. These electrons result from the interaction of gamma rays--which come from the fission process--with air. The electron cloud is analogous to a semispherically expanding antenna. Other independent processes, which account for the cancellation of the earth's electrostatic and magnetic field or for plasma oscillations

within the highly ionized region surrounding the burst, are computed to result in signal strengths which are small compared to those observed. It is believed, however, that these processes do cause minor perturbations in the EM signatures.

In order to establish the correct polarity in the electric field, an asymmetry must exist in the vertical plane of the detonation. This asymmetry is believed to result from either a ground interface, or for higher altitude bursts, from the atmospheric density gradient. This theory is reasonably well corroborated in that the signature for a ground burst is different in character from the signature of a burst for which the ionized sphere is large in dimension and the atmospheric inhomogeneity is significant. The EM signature differs from those for the ground burst characteristics (dependent upon yield) which would be observed up to a burst altitude on the order of 6000 to 12,000 feet.

As the range from the burst for EM signal detection increases, the specific details of the initial signature become less significant. At ranges less than about 200 nm (dependent upon yield), the signature characteristics can yield information on yield, staging times, and burst height. At distances greater than about 1000 nm, the signature

characteristics can no longer provide such detailed information. However, some measure of yield can be made from the amplitude of the EM waveform at distances greater than 1000 nm. In addition, the gross characteristics of the initial waveform can provide information on the altitude regime of detonation for distances of, say, 500 to 1800 nm.

1.3.2 General Characteristics of Signal. There are several characteristics of the electromagnetic signal which are pertinent to the considerations of the Polaris system.

The signal has large amplitudes. A signal strength of 5 volts/meter can be expected at 500 nm from a 200-kt detonation. At a distance of 2500 nm, a signal strength of 0.6 to 1.2 volts/meter can be expected. EM field strength is a function of weapon yield and altitude of burst.

The VLF prompt or ground wave portion of the signal is initially negative in polarity (for low altitudes). Multiple bounces from the D-layer modify later signals significantly.

The characteristic frequency of the signal is in the VLF range. Typically, the predominant frequency component ranges from 10 to 20 kc. The amplitude of the frequency components is down by an order of magnitude below 5 kc and above 40 kc (dependent on distance).

Interference between the ground wave and the sky wave can be noticed for ranges in excess of about 500 nm. At 2500 nm, the multiple-bounce sky waves are dominant.

The signals are sufficiently low in frequency that they are capable of reception under the surface of the ocean. It is expected that the VLF receiving antenna systems which are presently installed in Polaris submarines can be used for the IBDA function.

The signal can be detected at extreme ranges. This capability has been experimentally verified for receiving systems at the surface.

In preparation for these tests, waveforms recorded in previous operations from various yields, locations, and burst heights were analyzed for frequency content and amplitude-distance characteristics. Extrapolation of this previous data to the present test conditions allowed estimates of necessary recording equipment features and yield versus signal strengths to be expected. Attention is directed to References 6, 7, 8 and 9 as examples, plus significant data taken during this operation by Taylor, NBS; Lockwood, MITRE; and Theobald at LASL.

1.3.3 Signal Distortion. Most of the data recorded shows some variation in amplitude and wave shapes for similar shots. Several important factors contribute to

this observed variation. A study of the propagation of electromagnetic waves in a conductive media (such as sea water) reveals that the more significant factors affecting wave amplitude and phase distortions are conductivity, wave velocity, and the media intrinsic impedance. Figures 1.1, 1.2, and 1.3 are plots of these functions versus frequency for conductive media. An EM signal from a bomb is a transient signal containing a varied spectra of frequency components. The relative transfer functions of the various frequencies may be calculated through the data presented in the figures. Figure 2.8 illustrates the further distortion due to the varying range and D-layer ionospheric heights which were estimated to be typical of post-dawn conditions for most of the shots, although a few shots were early enough to have been transmitted along the South-North dawn region in the ionosphere and therefore are of some interest as a unique propagation path.

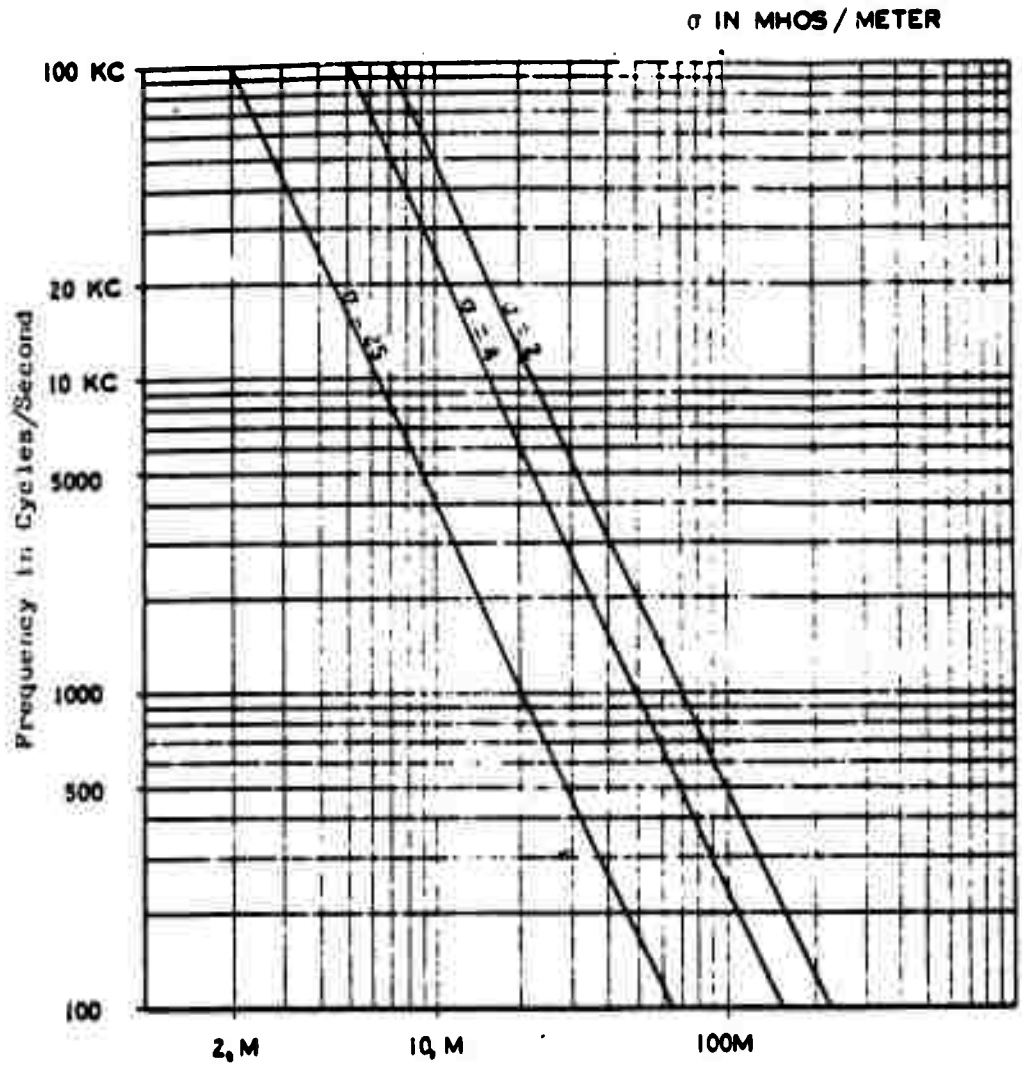

Figure 1.1 Electromagnetic wavelength in conducting media.

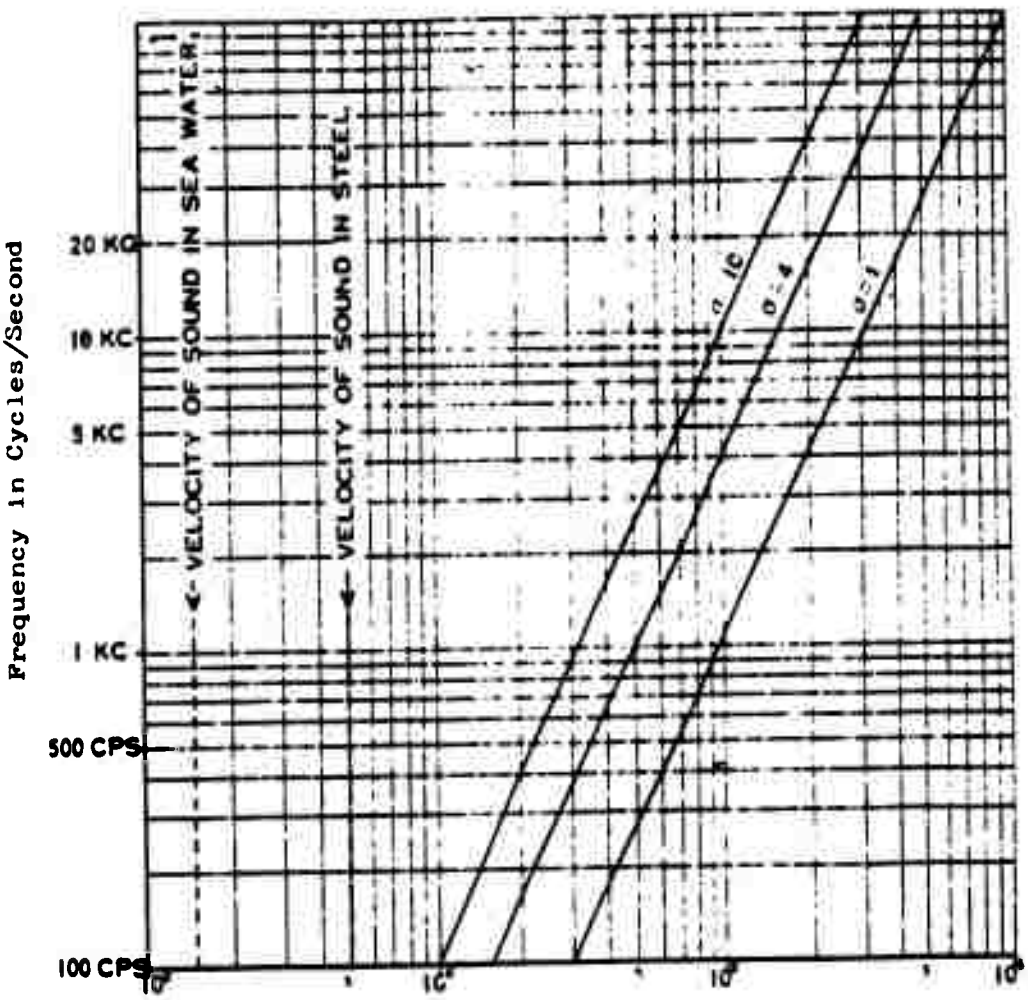

Figure 1.2 Velocity in conductive media.

$$\eta = \sqrt{\frac{\omega \mu}{\sigma}}$$

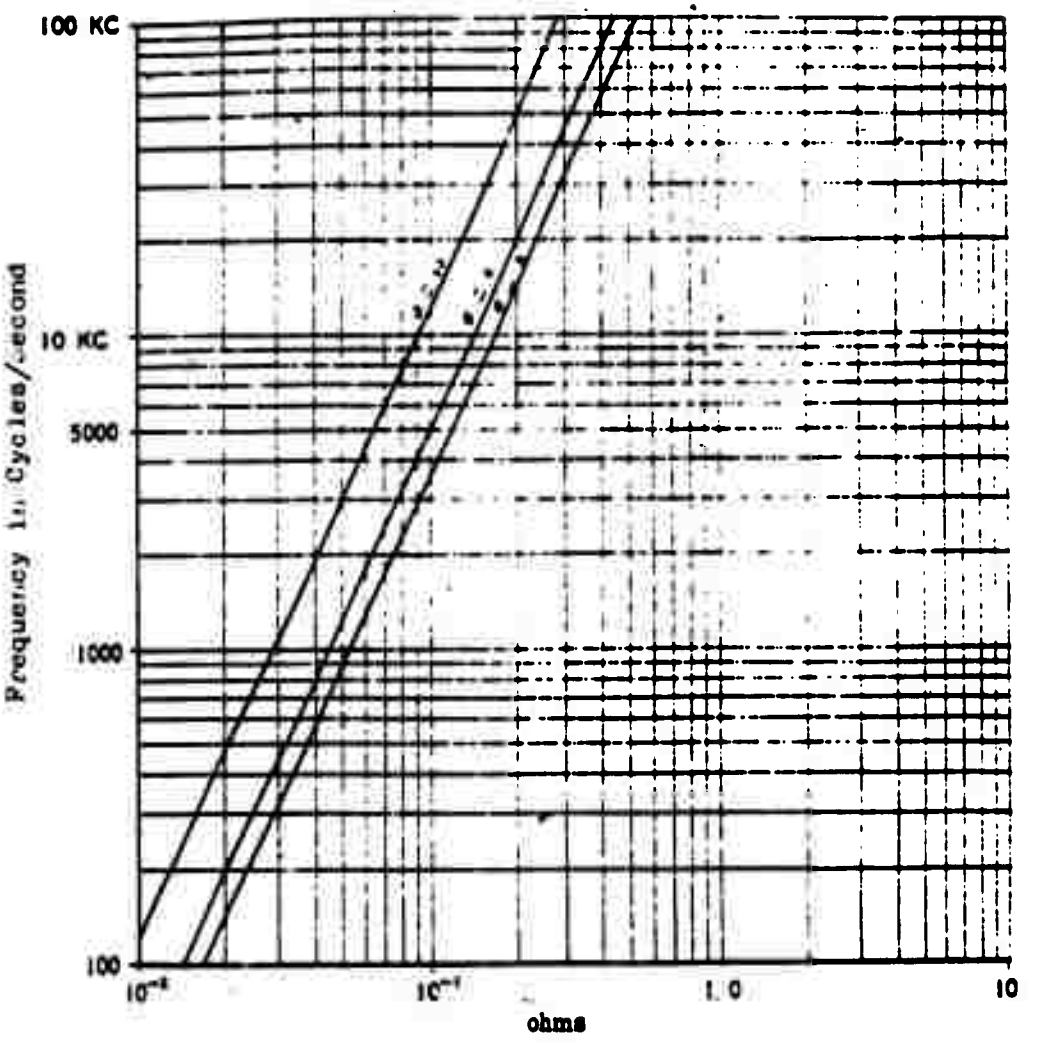

η INTRINSIC IMPEDANCE $\angle 45^{\circ}$

$\mu = 4\pi \times 10^{-7}$ PERMEABILITY

σ = CONDUCTIVITY (MHOS)

$\omega = 2\pi \times$ FREQ. (C. P. S.)

Figure 1.3 Intrinsic impedance.

CHAPTER 2

PROCEDURE

2.1 OPERATIONS

2.1.1 Shot Participation. Participation in all the shots of Operation DOMINIC was planned. Table 2.1 lists shots along with pertinent information. Included in the table are the pre-shot estimates of expected EM signal strengths at the test site (see Section 2.2.2).

2.1.2 Test Site Activities. The primary activity at the test site consisted of cruising on-station within 100 miles of Oahu and recording EM signals as scheduled. In pre- and post-shot intervals, calibrations were made, and atmospheric noise was recorded. Considerable time and effort were directed toward establishing communications with proper sources in order to coordinate ship movements and shot recording times.

2.2 INSTRUMENTATION

2.2.1 Test Site Installation. The installation for these tests consisted of two stations on ships cruising at slow speed in the coastal deep waters south of Oahu. The ships, operating as Task Element 8.3.6.6 were the minesweepers MSO-457 LOYALTY and MSO-456 INFLICT. Each vessel was outfitted with antennas both above and

underwater. Each antenna was operated into separate receivers, and outputs were recorded by two methods, on film and on magnetic tape. Block diagrams of the station layouts appear in Figure 2.1.

The instrumentation, i.e., antennas, amplifiers, and recording systems, was patterned very broadly after equipments used by NBS Central Radio Propagation Laboratory, Boulder, Colorado, with many important variations needed for this specific project. The variations will be noted in the following paragraphs.

The Antennas. The long floating wire consisting of 1000 feet of RG-298 was used in an approximation of a typical submarine installation, i.e., one end shorted to sea water by a MX-587/U and the other end connected through a waterproof seal (connector UG-1404/U) to RG-17/U center conductor. The outer shield of the RG-17 was also connected to the sea water by this special connector.* The pattern of this long floating wire is shown in Figure 2.2.

The loop antenna actually consisted of several

---

*This connector proved to be too heavy and bulky and actually broke the RG-298 antenna wire several times, so an alternate seal was devised by the ship's crew. No electrical changes were noted.

alternate loops--all built by Kaman Nuclear.* The various antennas are categorized as follows:

Large Loops

Mod 1, 2, 3	Identical, shielded, ten-turn loops, 6 x 6 ft square, wires spaced within the fiberglass shell to reduce capacitance.
Mod 4, 5	Same as Mod 1, unshielded
Mod 6	Same as Mod 4, 23 turns
Mod 7	Same as Mod 4, 47 turns

Small Loop, 18 x 19 inches, 17 turns

Mod 1& Mod 7	the small loops were used in the experimental testing and as an alternate to the long wire antenna or large loops whenever operational difficulties restricted use of these antennas.
Mod 2	antenna was damaged by the propeller on the first test run in heavy seas. Mod 3 was not received (lost in shipment from 7 March tc 20 May). The unshielded units Mod 4, 5, 6 were determined to be satisfactory since the conducting sea water acted as a shield and results duplicated the Mod 2 test results.

The experimental pattern of the Mod 4 loop antenna is shown in Figure 2.3 using Navy Station NPM as a source. The pattern agreement with the theoretical cosine pattern illustrates that the shielding and spurious pickup characteristics

*Design parameters were determined based upon consultation with NRL.

of the triple-shielded balanced lead-in cable was adequate This feature is an important consideration since the point of detection is above water in a high field strength, whereas the desired signal traveling down through the water is attenuated severely before being picked up by the underwater loop antennas.

The loop antennas normally have an effective aperture, described as an effective height, $h = \frac{2\pi NA}{\lambda}$ for

$N = 10$ turns

$A = 1.87^2 = 3.5$ square meters

$\lambda = 3 \times 10^4$ meters at 10 kc (or 16 meters in sea water, see Figure 1.1).

Therefore, above water

$h = .0074$

$h = .017$ for $N = 23$ turns

or underwater, due to the extreme change in wavelength

$h = 13.8$ for $N = 10$ turns

$h = 37$ for $N = 23$ turns

The above calculations are of casual benefit, since in the actual case, the vertically oriented submerged loop acts as a much better receiver on the side nearer the water surface, and the side which is deeper receives about 6 decibels (at 10 kc) less signal than the upper side and actually reradiates some of this signal (Reference 11).

Thus, the usual 90° phase lag is less than 24° at frequencies above 10 kc (illustrated by the following vector diagram) which explains why the observed phase shift is almost unnoticeable (about 7° at 19.4 kc) and why the effective aperture is more nearly that of the underwater antenna (see previous paragraph).

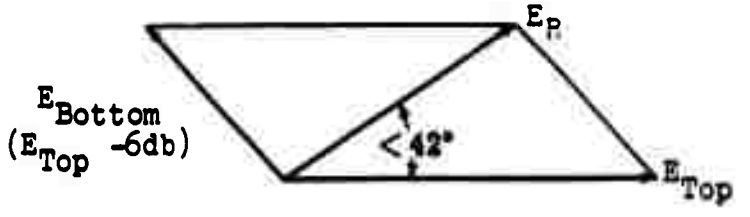

Phase delay between E_{Top} and E_{Bottom} is about 36° to 42° instead of almost 180° as for air loop.

Unfortunately, the tuned characteristics of the URM-6 input made direct comparison with the calibration loop very questionable, but the curves of depth versus attenuation as measured indicate that the antenna had an effective height of twice that of the calibration loop at the surface, and an above-water gain of about 10 decibels relative to the calibration loop.

The self-resonant frequency of the loop antenna Models 1 through 6 were all above 50 kc including the capacity of the long lead-in balanced cable.

Recording Equipment. Some amplification of the received signal was necessary in order to provide oscilloscope deflection of sufficient amplitude for film recording and reliable triggering. The amplifiers built at Kaman Nuclear were based on a circuit developed at Dartmouth College for use in the investigation of atmospherics or whistler during the IGY program (Reference 10). The detailed circuit of the amplifier is shown in Figure 2.4. It is to be noted that the amplifier has two input configurations: (1) a transformer input to a grounded-grid stage to approach a match for the very low impedance of the underwater loop antenna, and (2) a high-impedance input stage to be used with the whip above-water antenna.

The amplifier characteristics include variable gain up to $88 \times 10^3 \ (V_{in}/V_{out})^{\frac{1}{2}}$ plus high and low signal inputs, low noise and hum bucking, and input balancing control. Typical frequency response curves are shown in Figures 2.5 and 2.6. Printed circuit techniques were used to simplify construction. Excellent isolation of output from input was also achieved with the printed circuit; this feature is necessary with a high-gain circuit in order to avoid oscillation or regeneration. Figure 2.7 is a photograph of the receiver-amplifier, power supply, and signal simulator or calibrator with water-tight cabinet

on the amplifier. Figure 2.8 shows a comparison of the output-input frequency characteristics of the receiver. The signal seen was generated by the simulator and is comparable to a spheric or EM signal.

The power supply for the amplifiers includes a direct-current filament supply and a well-filtered, high-voltage output. The circuit diagram of this component is shown in Figure 2.4.

The time of arrival of the EM signal of a given shot at the two recording stations was used to reduce the data analysis required in an environment containing a possible high incidence of spherics of large magnitude and to reduce equipment running time. Advance knowledge of shot time and countdown reception, in those cases where available, reduced the data collection time to a minimum. In order to utilize post-shot time to confirm the reduced data and, if necessary, to further pinpoint the signal on the record (film or tape) which also carried spheric signals, timing instrumentation was installed. This equipment was built to utilize WWVH transmission, U.S. Navy VLF station transmission, and voice countdown transfer to tape. Synchronization of clocks with WWVH was made prior to tests; these clocks were then photographed on the same film as the EM signal.

Voice radio countdown was received from Johnston Island, 3A3 emission, 15 kw on high-frequency channels for the FISH BOWL events.

Countdown information was not available on the Christmas Island events (except for Frigate Bird). Data was recorded on these events using the predicted shot time only, plus coded messages on the Navy Task Group 8.3.7 transmissions.

An increase in the reliability of the signal-recording installation was achieved by the redundancy built into the system. Two recording channels were available for each antenna used in the experiment. An oscilloscope strip film recording camera and a magnetic tape recorder channel were used in parallel. Another advantage of the two channels was that of dynamic range overlap from one channel to the next; this prevented the loss of data from the saturation of one channel.

The oscilloscopes were standard 551 Tektronix types; the oscillographic recording camera was a Dumont 321, of which three were available. This camera recorded oscilloscope traces on continuously moving 35-mm film; film motion was perpendicular to the scope sweep and was run, on the average, at a rate of 40 to 50 inches per

minute when high spheric levels were present and at 14.8. inches per minute during quiet periods.

The tape recorders were modified Viking 86 Stereo type which recorded two channels simultaneously. Alterations to the standard recorder preamplifier circuit and increase of tape transport to 15 inches per second yielded improved frequency response to about 17 kc.

2.2.2 Calibration Procedures.

General Signal Calibration. In Figure 2.1, the station block diagram, the three blocks labeled "Signal Simulator, WWVH Receiver" and "URM-6 VLF Field Strength Measurement Receiver" represent the on-board equipment used in the calibrations of data taken during the tests. These equipments made possible amplitude, phasing, and time calibrations.

Signals from the WWVH receiver, as mentioned in Section 2.2.1, were superimposed on the records, and allowed an accurate post-test location of the signal on both film and tape.

Since U.S. Navy VLF signals were being transmitted almost continually during the tests, they were used for amplitude calibration of the recorded shot signals. The URM-6, a precision VLF field strength receiver, was used on each ship for this purpose. Before and after each shot,

the 19.8-kc transmissions from NPM, the U.S. Navy VLF station located at Lualualei, Oahu, were recorded on tape and film using the EM signal recording equipment. The field strength of NPM was measured and recorded with the URM-6 during the same time period. A later comparison of the NPM signal amplitude to that of the shot signal, taking into account possible differences due to the frequencies involved and antenna bearings, yielded accurate information on the EM signal strength.

To insure uniformity on both ships, the URM-6 receivers were calibrated with the facilities available at QEL, and at the University of Hawaii, where Dr. Ralph Partridge had a precisely calibrated standard length antenna. The standard antenna and NPM transmissions were used as a check on the URM-6 dial settings.

The signal simulator was used to check polarity and gain of the system amplifiers with a signal approximating that generated by a shot. Scope triggering levels were adjusted using the signal simulator (equipment limitations were experienced in this operation).

Lightning or spherics within at least 1000 miles furnished additional data on the distortion of the signal as a function of depth. The monitoring of lightning

signals also assisted in determining the level of interference to be expected during listening periods aboard a submarine. Spheric activity in the area was quite high, and much useful data was recorded.

As a further aid in setting oscilloscope gain controls, the EM signal strength expected from each shot was calculated in advance. The nomograms of Figure 2.9 were used for the pre-shot signal estimate. By a summation of ground, one-, two-, and three-hop signals with arrival times given in the nomogram, and having previous knowledge of signal strengths generated by weapons (References 6,7,8, 9), the signals at the test site were pre-calculated.

Computations used in setting up the nomograms were:

t_n = time, seconds

D = distance

H = D-layer height

t_o = ground wave

$t_o^2 = (1.11 \times 10^{-11})D^2$

t_1 = one-hop time

$t_1^2 = (1.11 \times 10^{-11})D^2 + (4.44 \times 10^{-11})H^2$

t_2 = two-hop time

$t_2^2 = (1.11 \times 10^{-11})D^2 + (1.778 \times 10^{-10})H^2$

t_3 = three-hop time

$t_3^2 = (1.11 \times 10^{-11})D^2 + (4 \times 10^{-10})H^2$

Underwater Antenna Calibration. Depth versus attenuation measurements were made in deep (2-mile) and shallow water. The electrical (phase shift) depth was used, since the actual depth was a function of wave structure, line-rigging uncertainties, and streaming effects at towing speeds required in rough water (over 4 knots). Sharks restricted swimmer activity so that actual measurements were not made during shot exercises. Figures 2.10 through 2.13 illustrate the attenuation versus depth as a function of frequency, define the effective loop gain, and reveal the noise-reducing characteristics of underwater antennas.

The variation in results indicate that probably other effects influence the received signal, such as a variation of antenna gain and match to the amplifier with frequency when the antenna is immersed in sea water, in addition to the uncertainty of absolute depth at the instant the measurements were made. Another variable was the angular positioning uncertainty of the antenna for signals from Navy Stations NAA, NPM, and NPD which were used as inputs for depth attenuation measurements as noted in Figures 2.10 through 2.13.

Page 31. Deleted

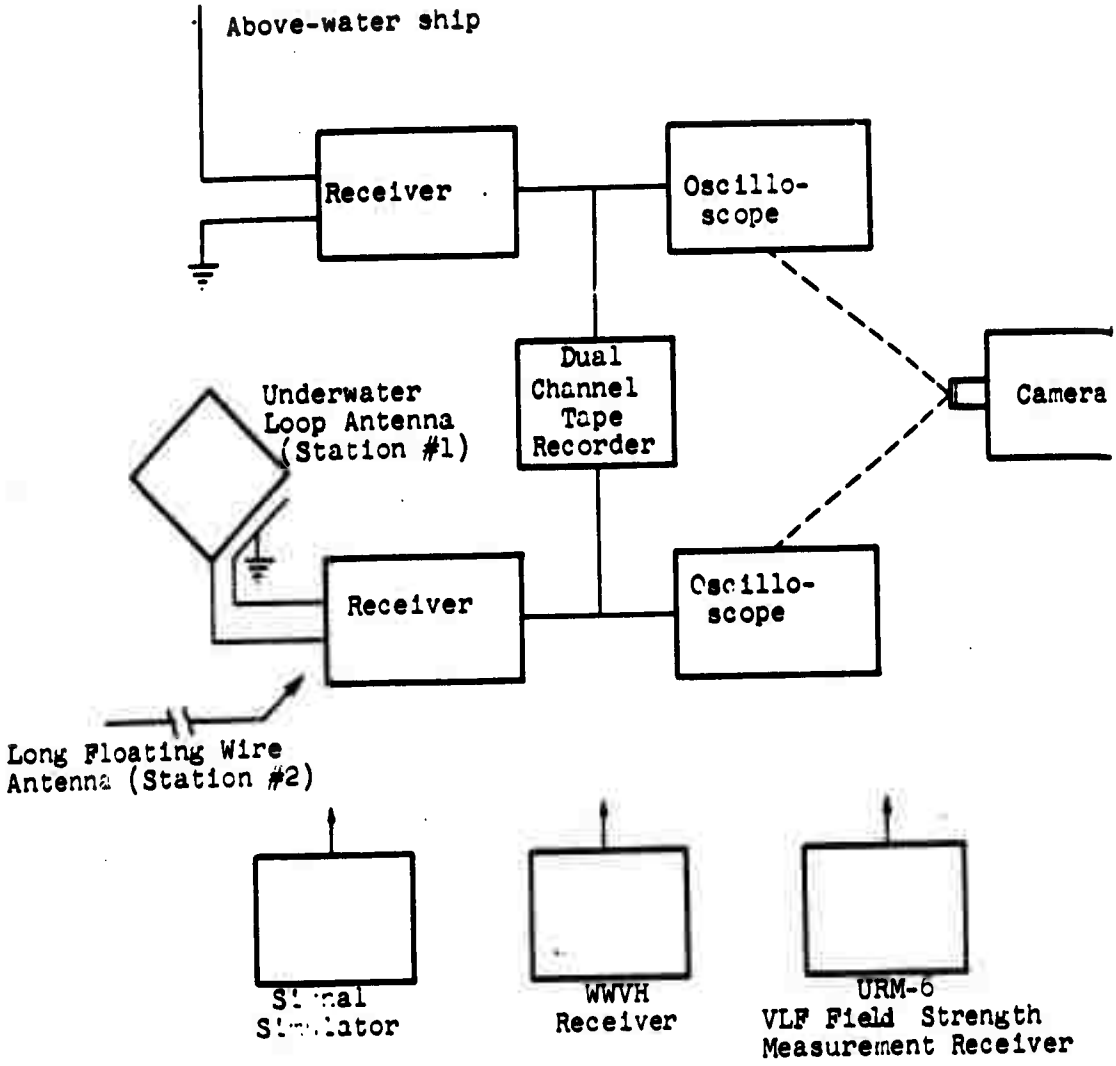

Figure 2.1 Block station diagram.

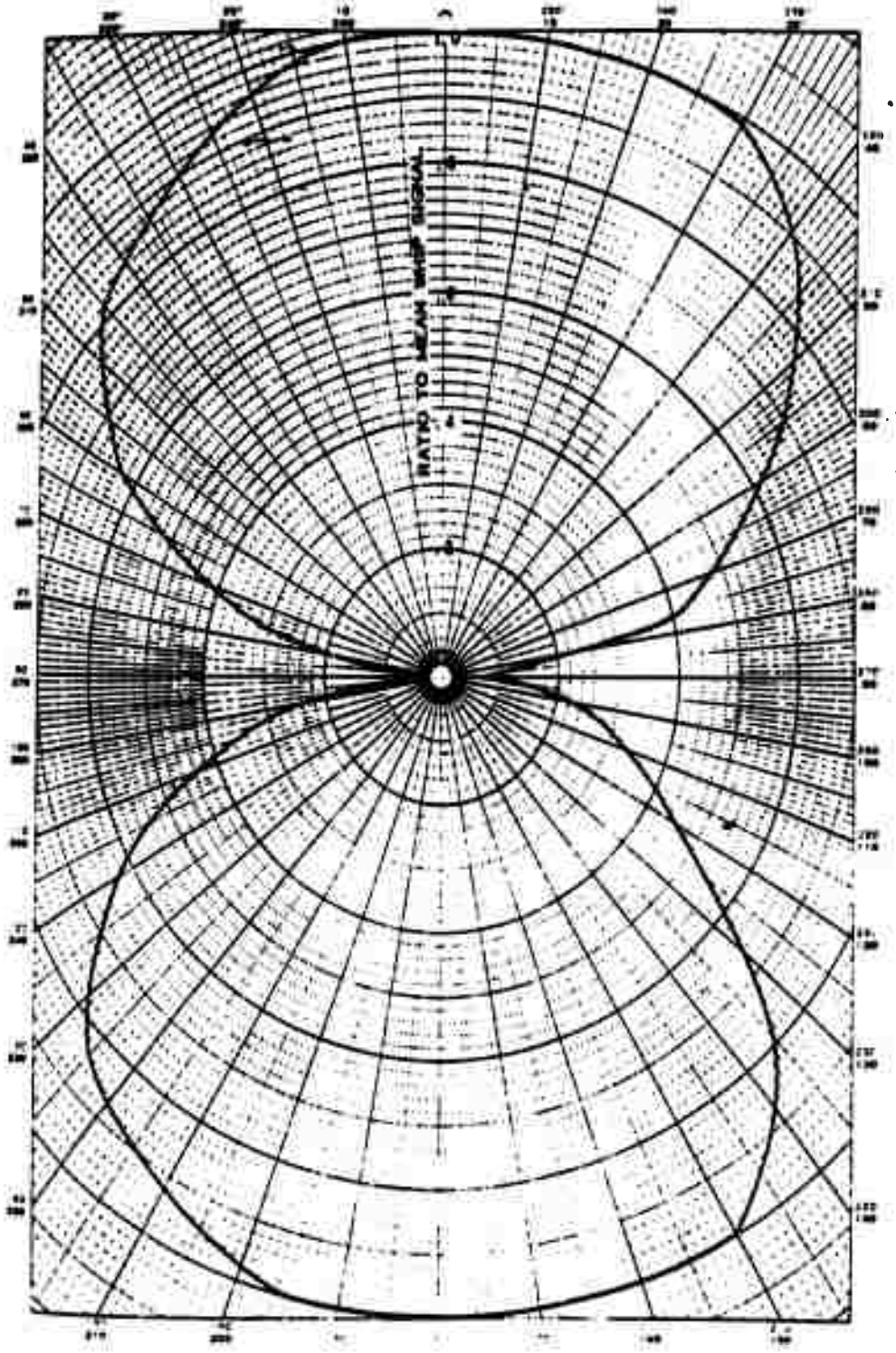

Figure 2.2 Wire pattern on NPM, 19.8 kc, 6 June 1962, bearings relative.

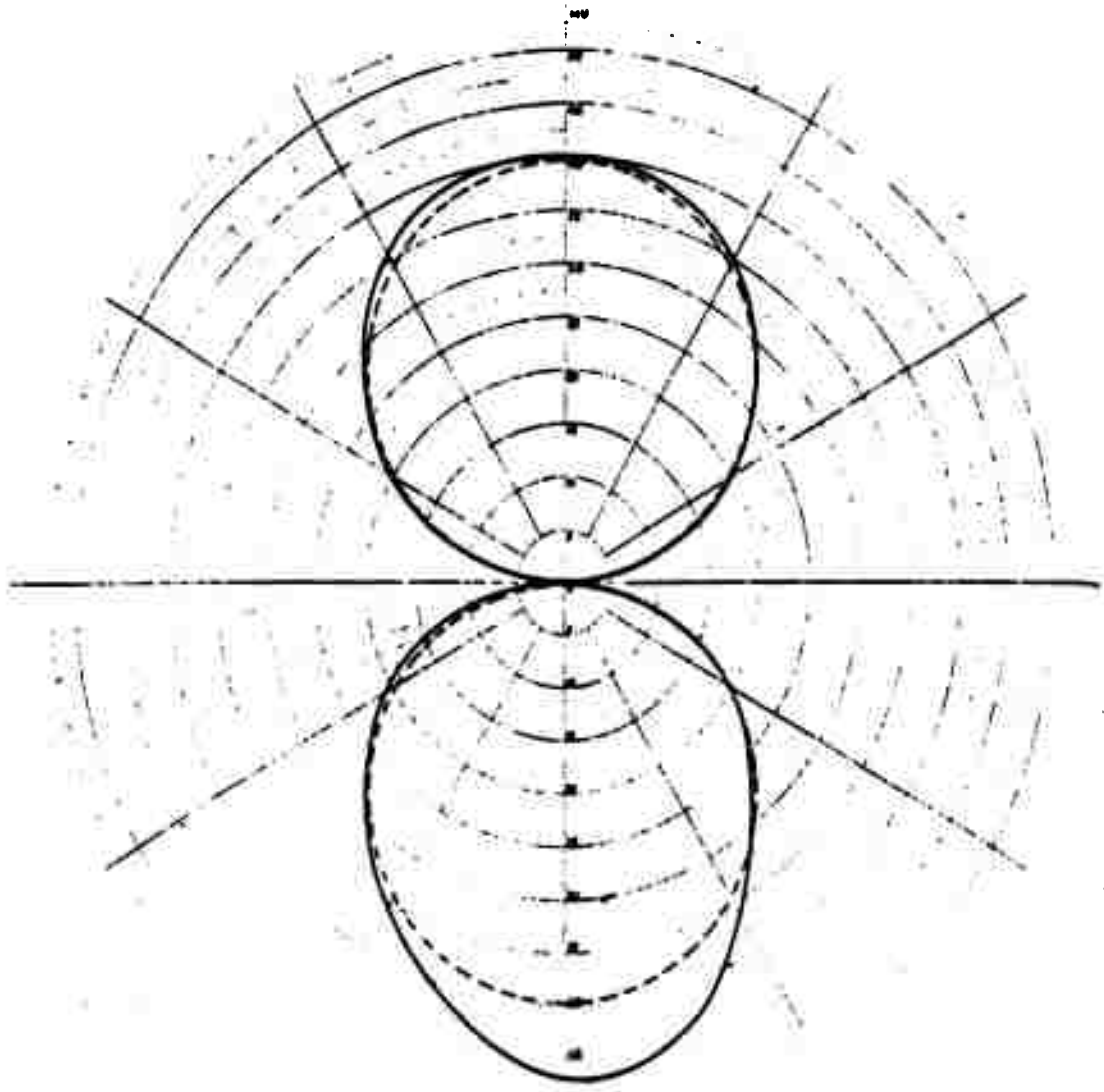

Radial scale in millivolts

Voltage Plot NPM
Effective Depth to Loop ≈ 2½ Fathoms
Apparent Distortion Due to Ship at 180°. Antenna 150 ft.
Astern is ..6 db. No Distortion Over ± 120°.
—— Actual ---- Cos θ Theoretical

Figure 2.3 Underwater loop pattern, Mod 4 antenna.

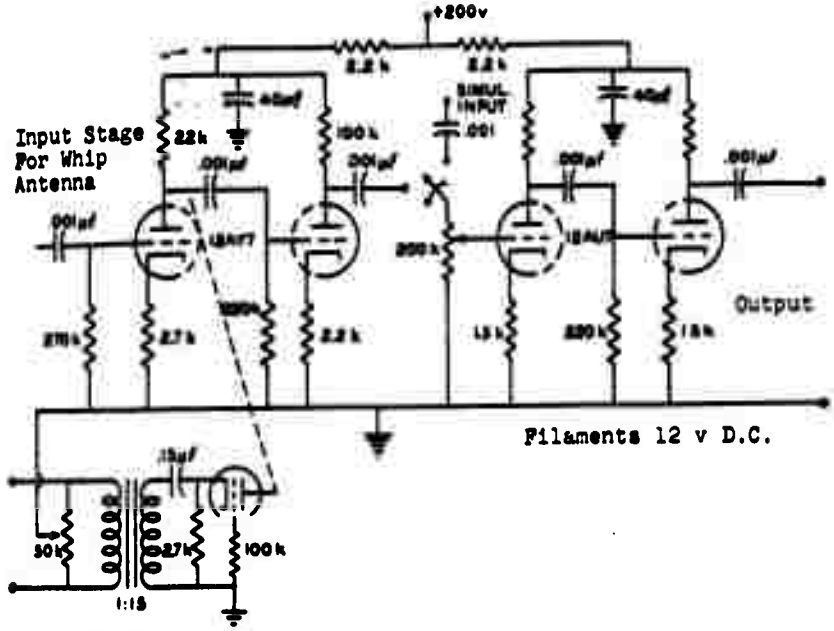

VLF BROADBAND RECEIVER-AMPLIFIER

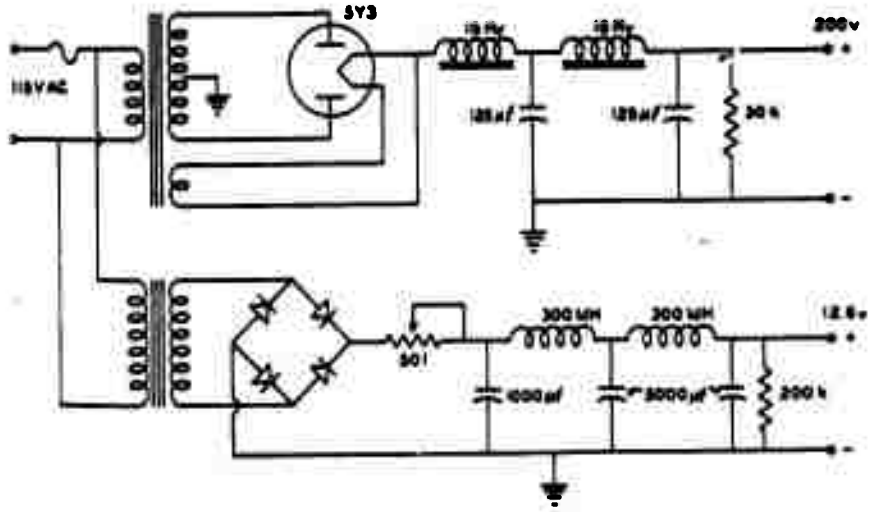

RECEIVER POWER SUPPLY

Figure 2.4 VLF broadband receiver.

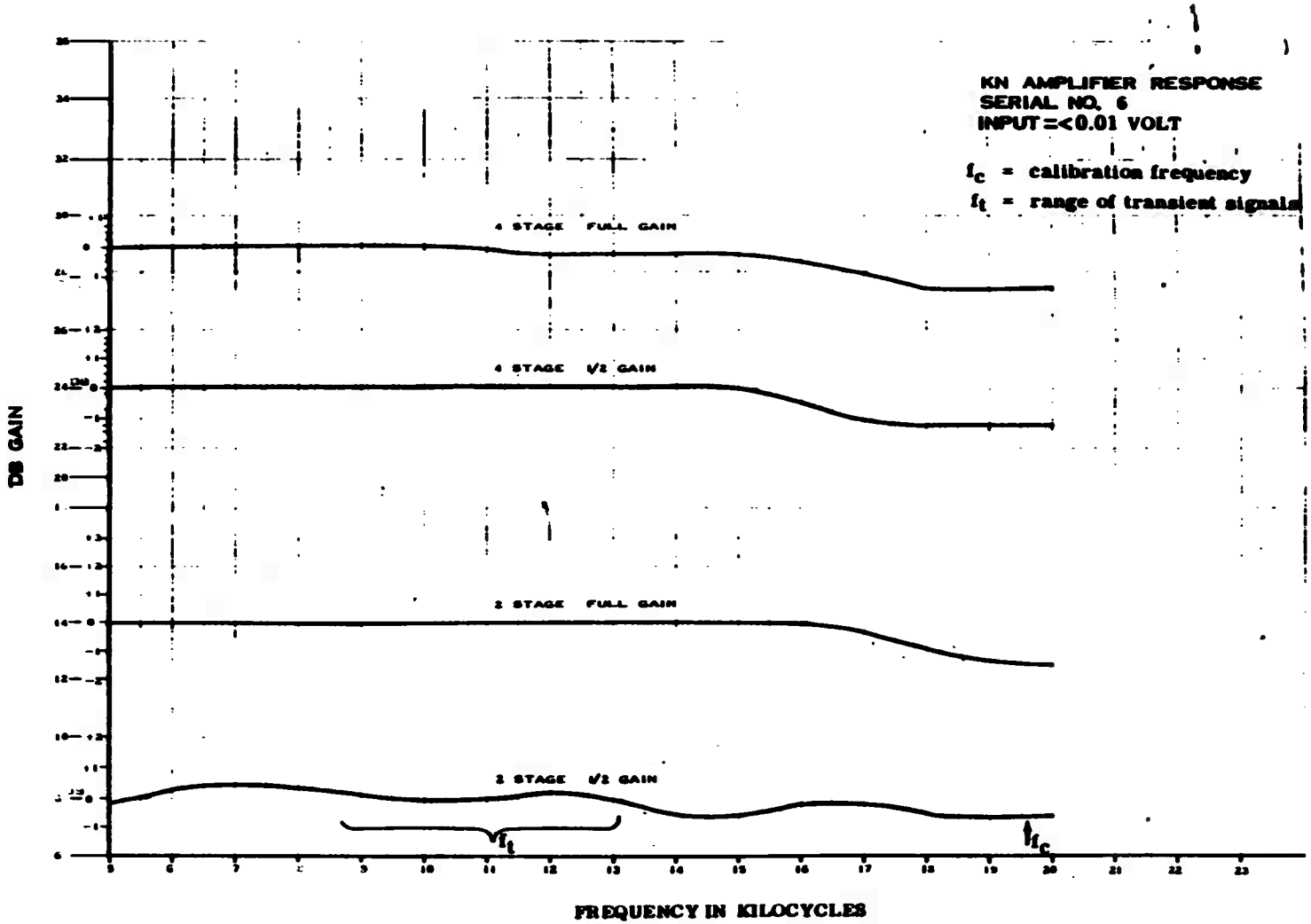
KN AMPLIFIER RESPONSE
SERIAL NO. 6
INPUT =<0.01 VOLT
f_c = calibration frequency
f_t = range of transient signals
4 STAGE FULL GAIN
4 STAGE 1/2 GAIN
2 STAGE FULL GAIN
2 STAGE 1/2 GAIN
DB GAIN
f_t
f_c
FREQUENCY IN KILOCYCLES

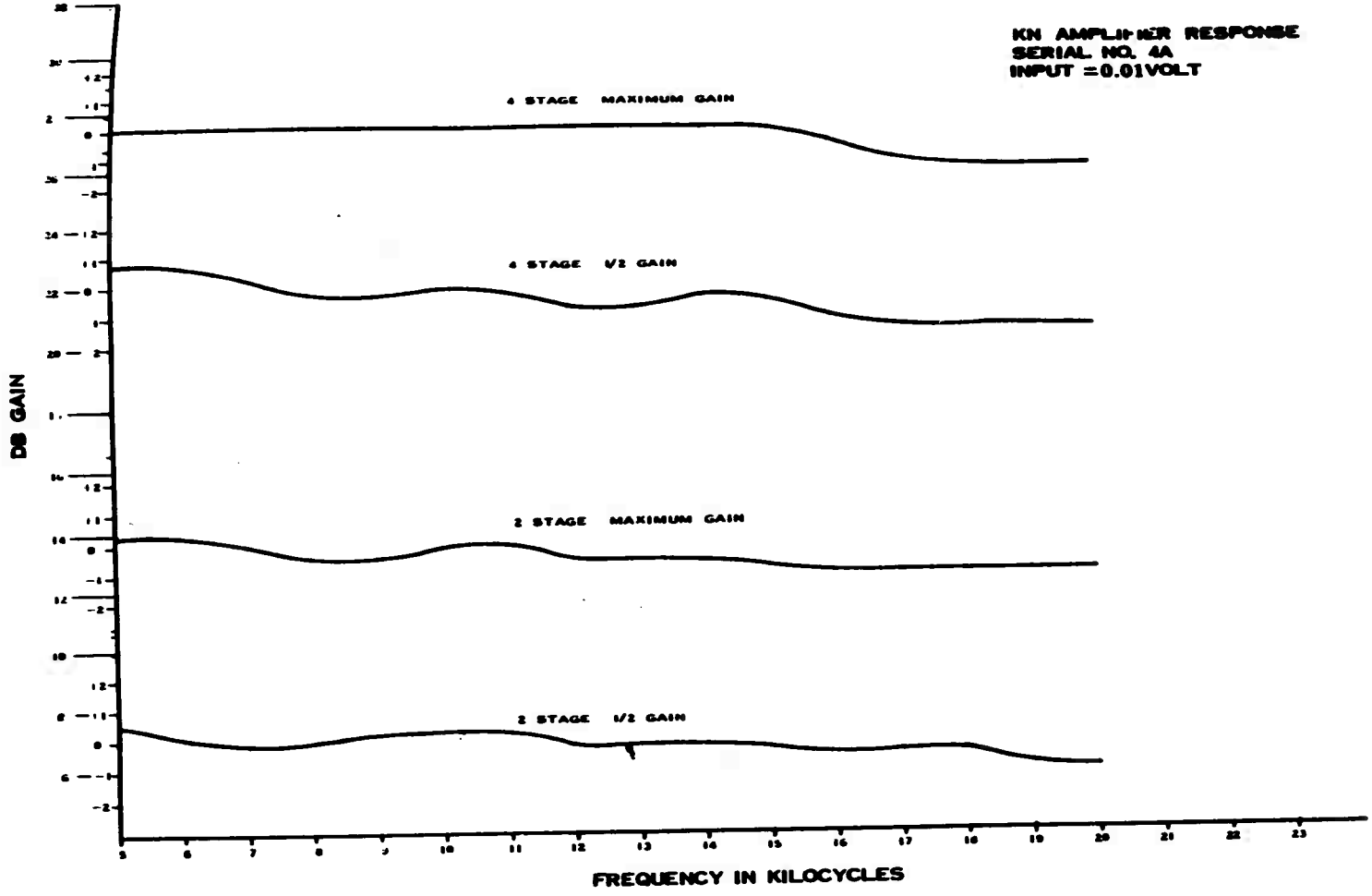

Figure 2.6 KN amplifier response, Serial No. 4A.

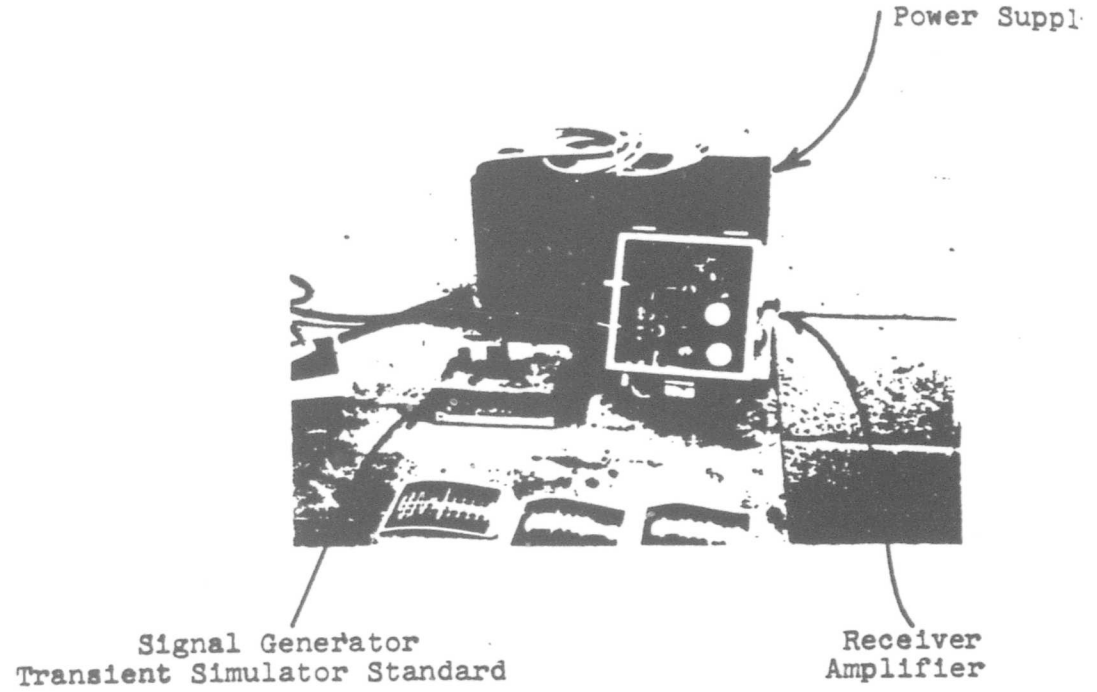

Figure 2.7 EM signal simulator and receiver.
(Kaman Nuclear photo)

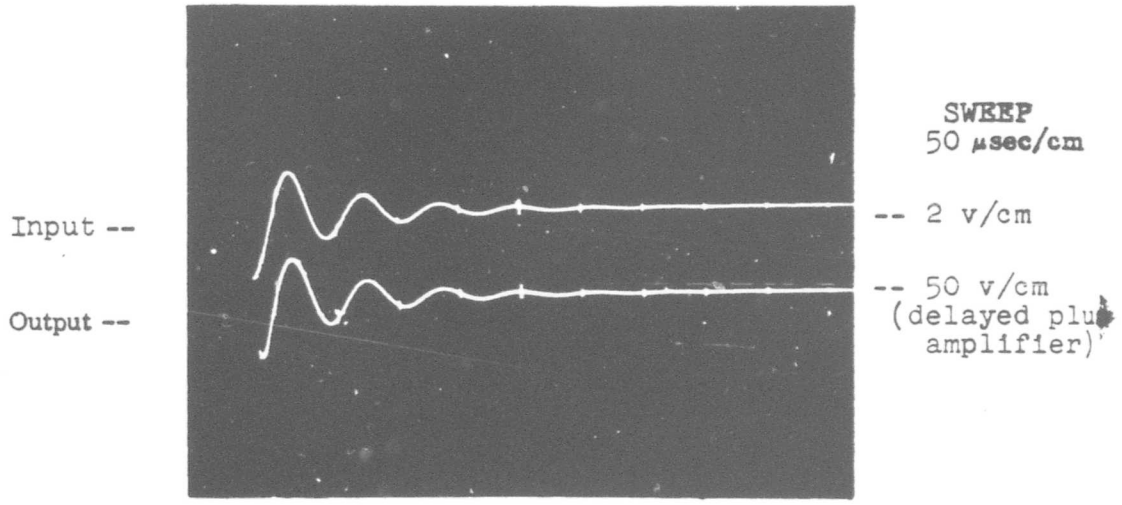

Figure 2.8 Output of simulator.

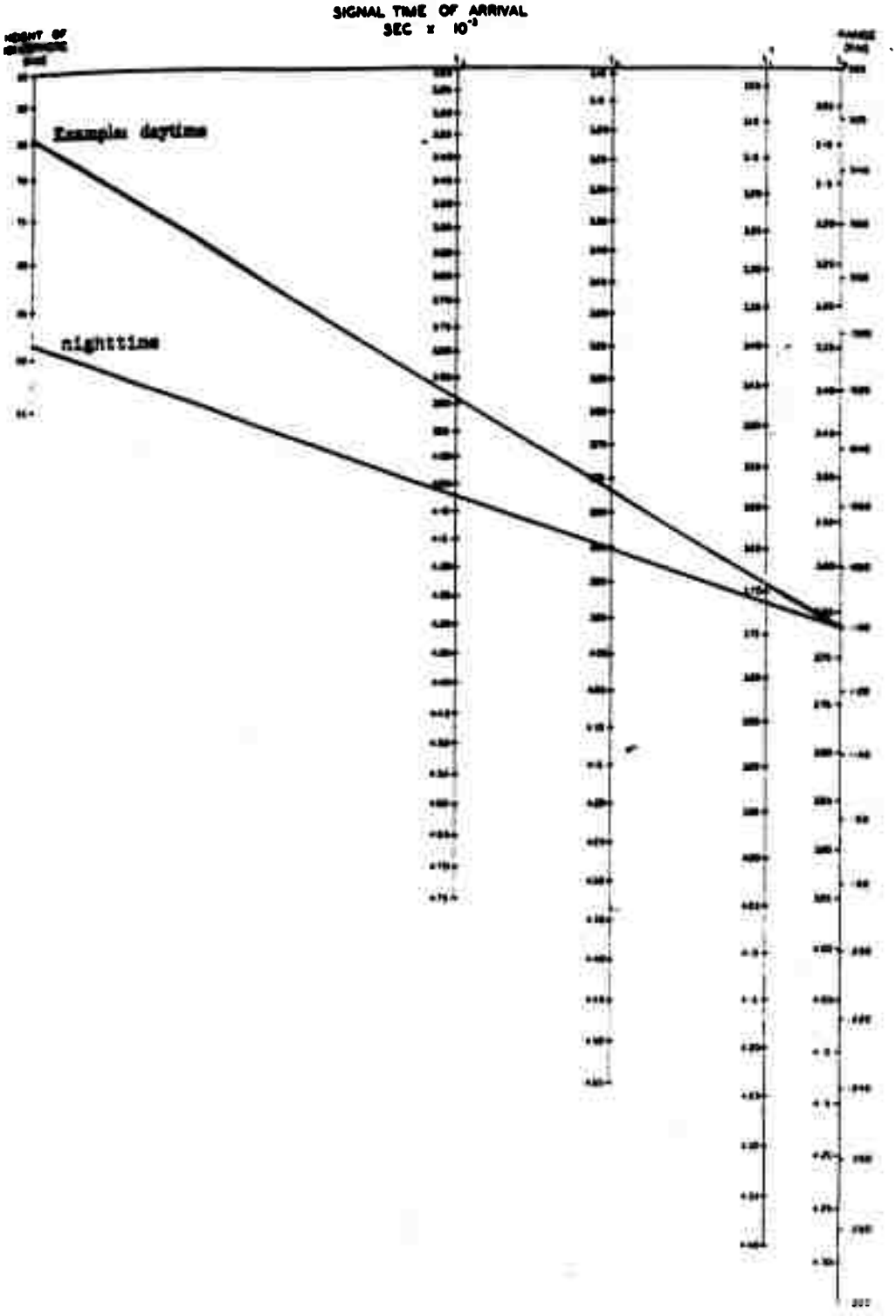

Figure 2.9 Nomogram for time of arrival of EM signal as a function of D-layer height and range.

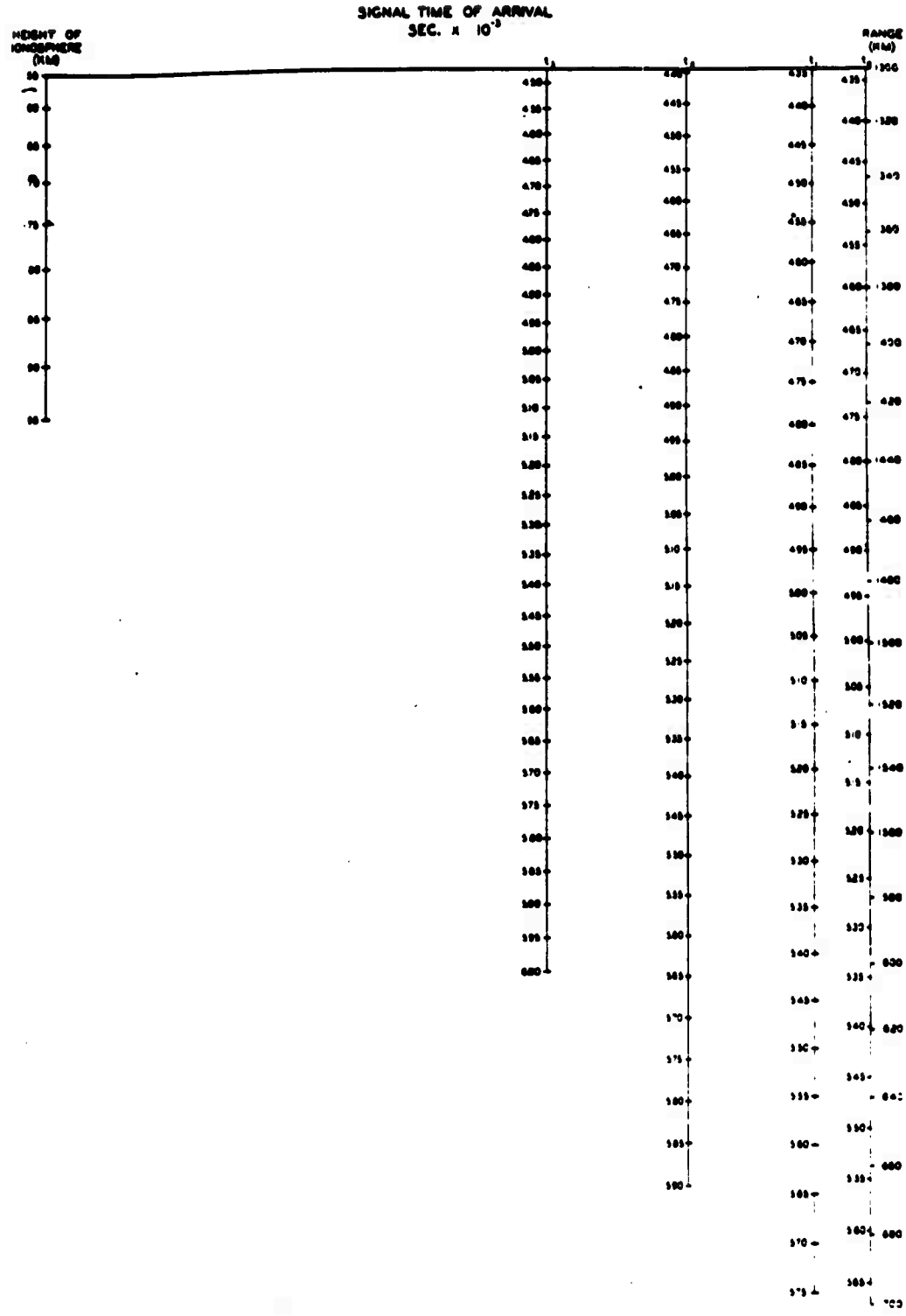

Figure 2.9 Continued.

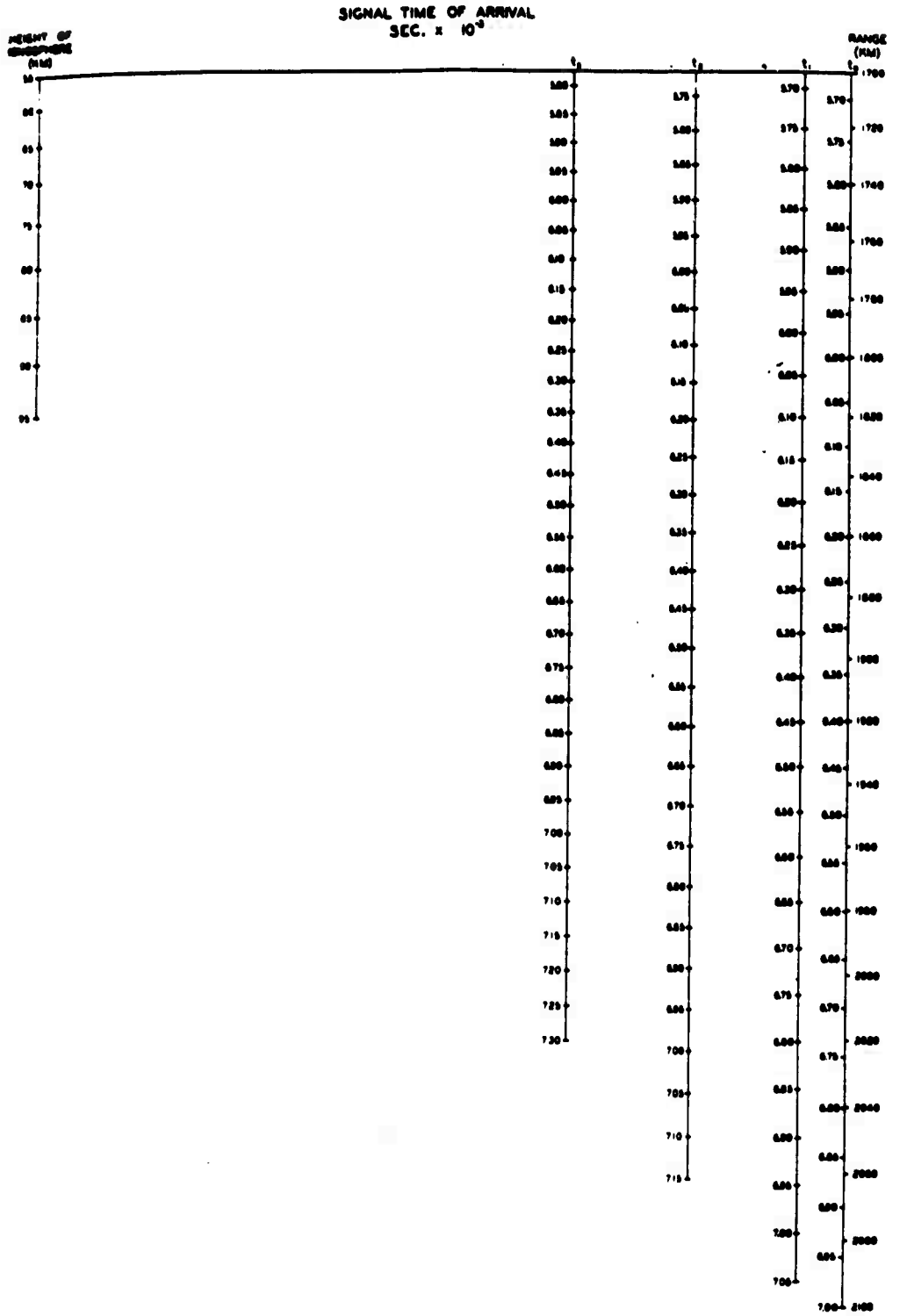

Figure 2.9 Continued.

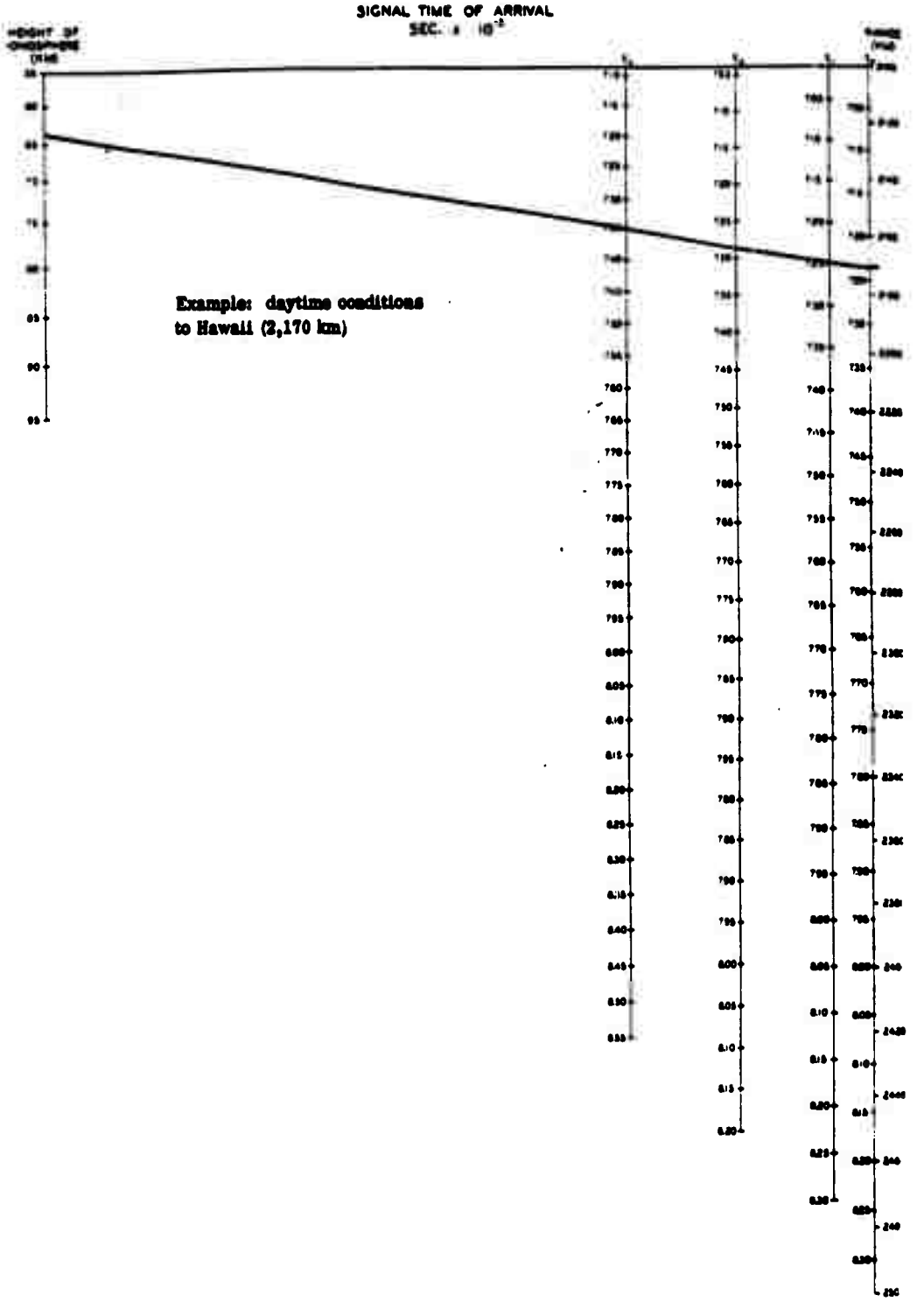

Figure 2.9 Continued.

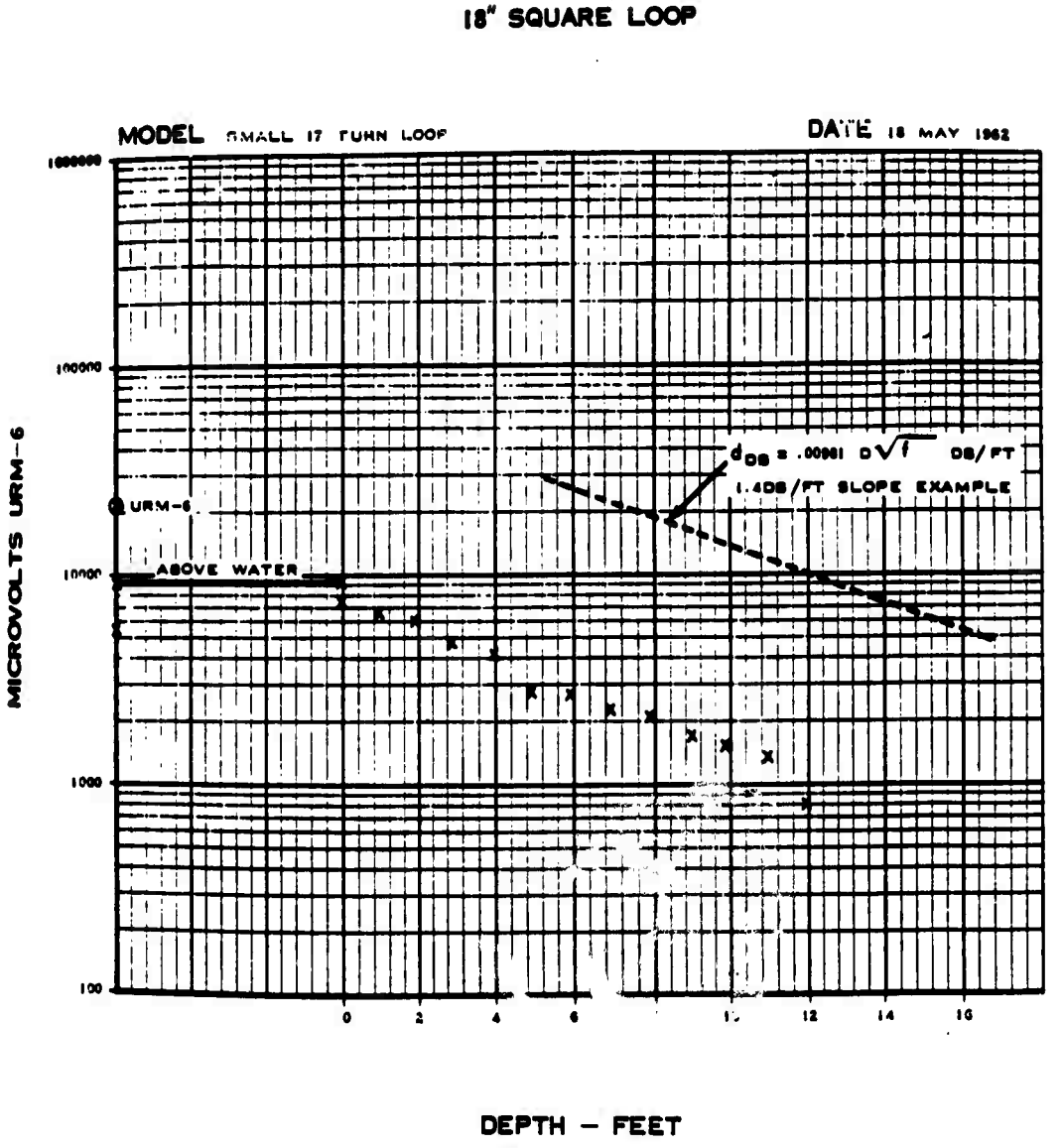

Figure 2.10 NPM depth/attenuation.

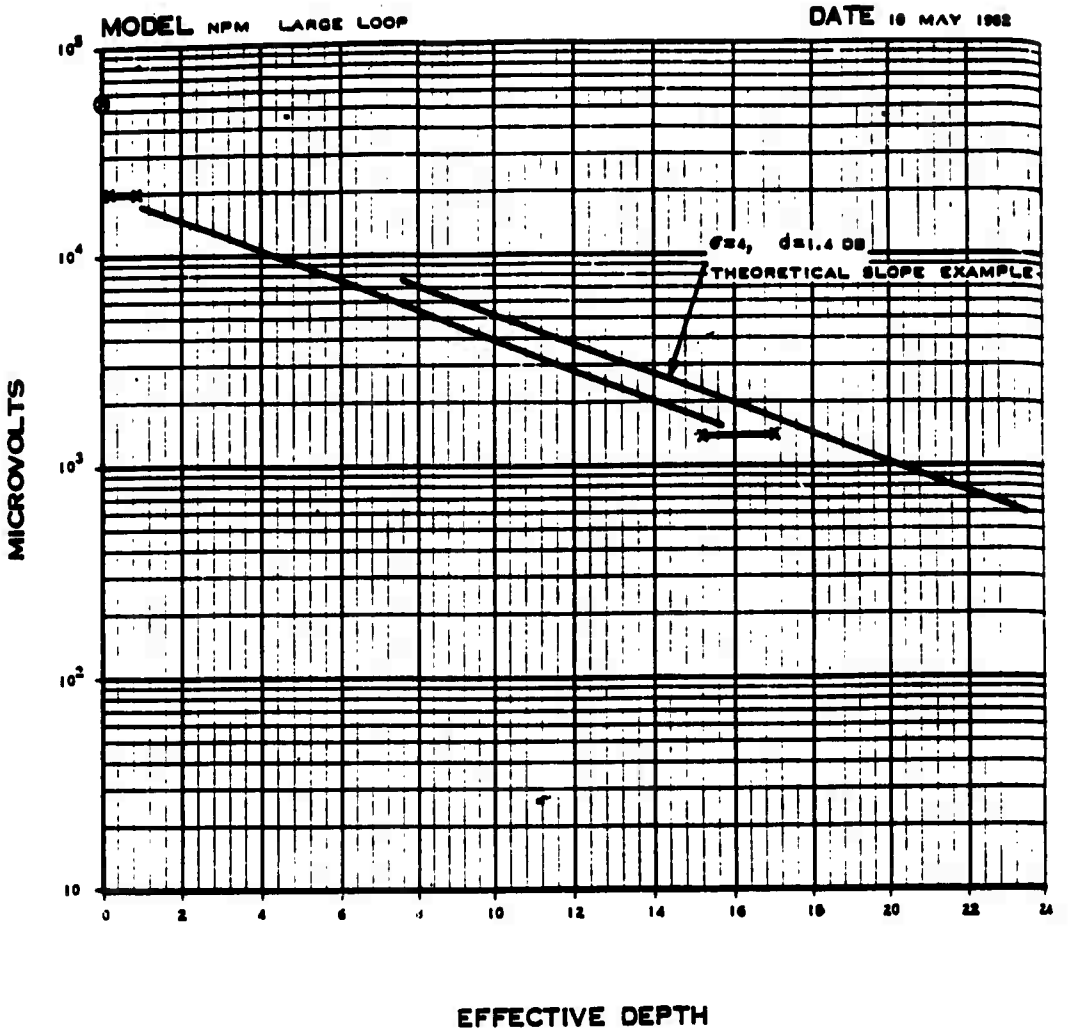

Figure 2.11 NPM attenuation versus effective depth.

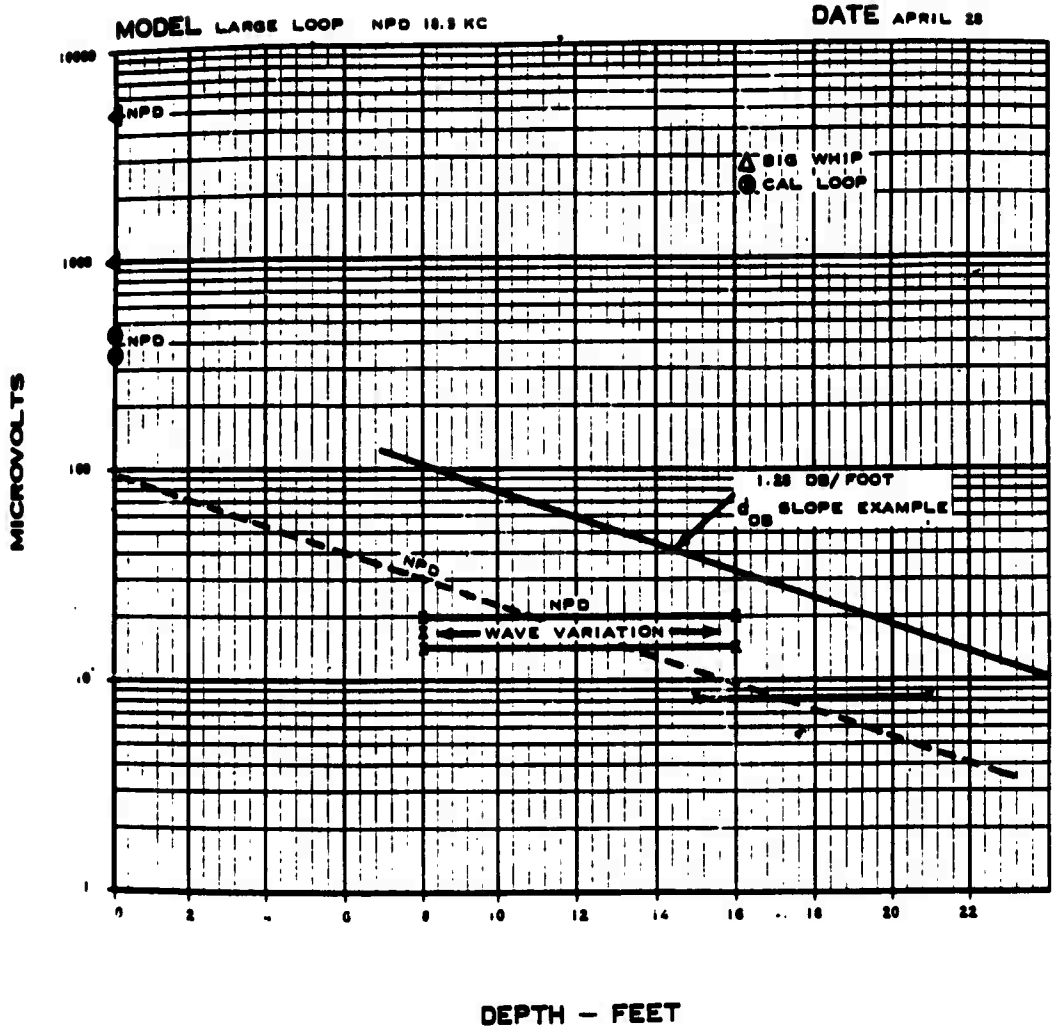

Figure 2.12 NPD attenuation versus depth.

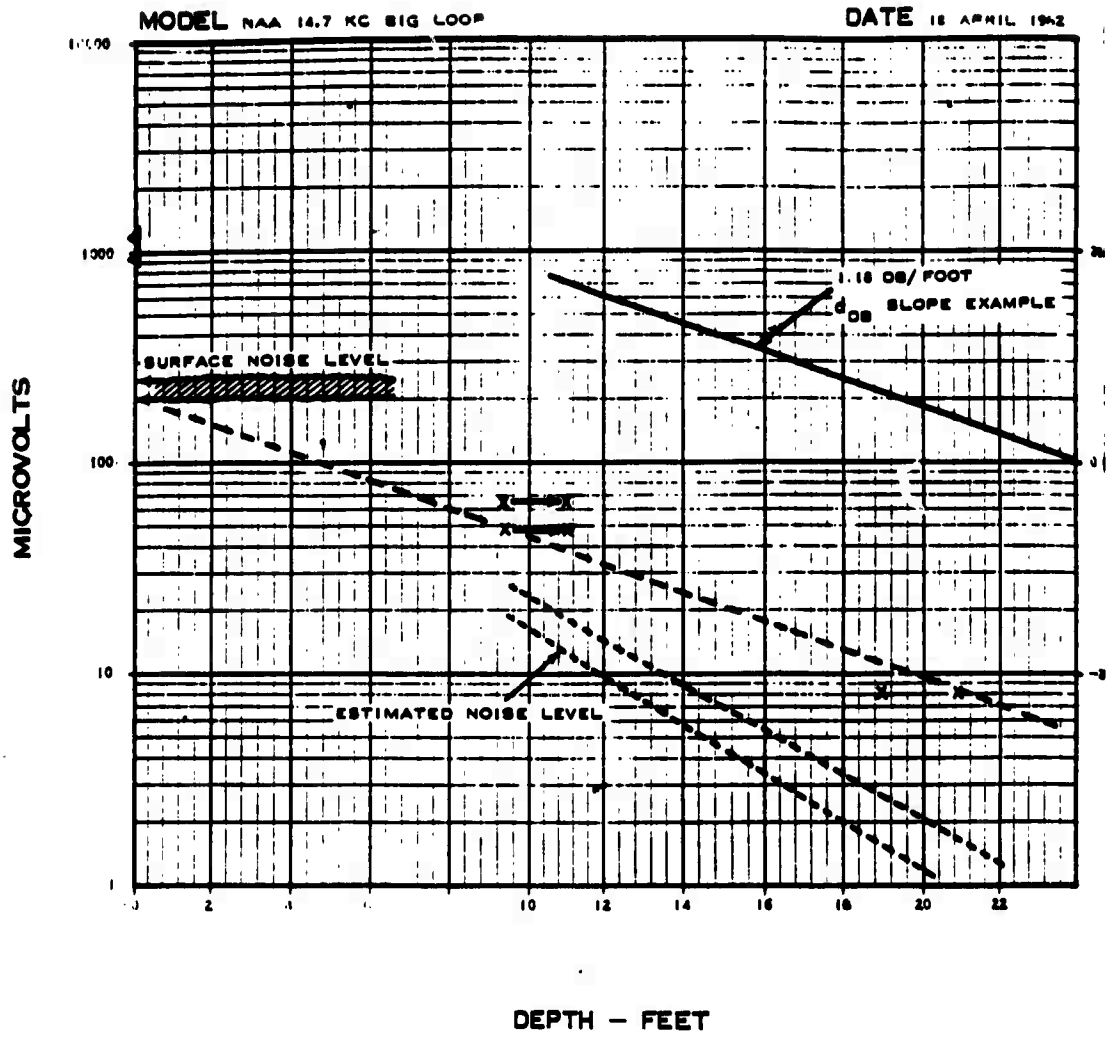

Figure 2.13 NAA attenuation versus depth.

CHAPTER 3

RESULTS AND DISCUSSION

Data was successfully recorded on 22 of the 26 shots listed in Table 2.1 which produced EM signals. Of the four shots for which no data was obtained, one (Tanana) had such a low yield that the signal could not be detected in the presence of the high noise level* at the test site at the time. A second shot (Star Fish Prime) completely saturated recording equipment so that no definable trace was obtained. Two shots (Aztec, Sunset) were not recorded because of miscoordination in communications about event timing.

The film data on 13 of the 22 recorded shots has been used to calculate field strengths of the EM pulses. Insufficient scope deflection, loss of calibration data, or improper triggering of the scope sweeps caused nine film records to be unreliable with respect to data analysis.

Since the tape recorders used were of low quality in phase and amplitude response in the desired frequency

---

*Loran station within line of site in bay where we sought shelter after experiencing 57°-roll weather!

range, the tapes were not analyzed for EM signal strengths. The tapes, however, produced a considerable quantity of information on spheric levels and other interferences one might encounter in attempting to differentiate an EM signal in the same time intervals.

Table 3.1 is a resume of EM pulse records obtained by Project 7.1 during the tests. The tape and oscilloscope records from each ship are listed separately. The figures listed by each record are of the traces which were photographed directly or transferred from a tape to film.

Figures 3.2 through 3.19 are reproductions of oscilloscope traces of the EM signals of shots listed thereon.

Signal strength is listed on the figure alongside the trace, if scope deflection was sufficient to allow the calibration. The method of calculation of the signal strengths is given below. (Also see Figure 3.1.)

1. NPM was used to calibrate the system at 19.4 kc.
2. NPM "at location" was measured with the URM-6

field strength receiver.

3. The intermediate amplifier was essentially flat from 5 kc to well above 25 kc (**Figures 2.5 and 2.6**).

4. The vertical whip signal as displayed on the scope represents the recorded equivalent level of NPM field strength. The actual input is modified by the whip's effective aperture, cable attenuation, and preamplifier gain. These factors do not enter into the calibration except as they are frequency dependent.

5. The effective height of the antenna

$$H_e = \frac{\lambda}{\pi \sin(\frac{2\pi h}{\lambda})} \sin^2 (\frac{\pi h}{\lambda})$$

h = 12 ft, whip = 3.7 meters

Case "A" λ_c = NPM = 15.5×10^3 meters

Case "B" λ_{10} kc = 30 km

ratio $\frac{He\ (10\ kc)}{He\ (19.4\ kc)}$ = 1.0 (within 1% accuracy)

The vertical whip is presumed to have an omni-directional pattern at these frequencies, although some variation was noted as the ships were rotated.

6. The attenuation in 35 feet of RG-58/U is negligible. The cable capacity of 28.5 pf/ft introduces a reactance of (1000 pf).

$$X_c \text{ (19.4 kc)} = \frac{1}{WC} = -j8.2 \text{ K}\Omega$$

$$X_c \text{ (10 kc)} = \frac{1}{WC} = -j16.2 \text{ K}\Omega$$

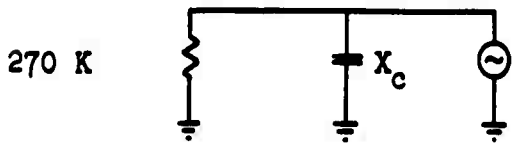

$K\ell = \frac{2\pi h}{\lambda}$ - the electrical length

(19.4 kc) $k = 15 \times 10^{-4}$

(10 kc) $k = 7.74 \times 10^{-4}$

The antenna impedance is

$$Z_{19.4} = 1/2[(20)(k\ell)^2 - j\ 120\ (k\ell)^{-1}(\log \frac{2\ell}{a} - 1)]$$

$$= 1/2(.000045 - j\ 39.6 \times 10^4)$$

$$= 45 \text{ } \mu\text{ohms} - j\ 396 \text{ K}\Omega$$

$$Z_{10} = 1/2(.000012 - j\ 76.8 \times 10^4)$$

$$= 12 \text{ } \mu\text{ohms} - j\ 768 \text{ K}\Omega$$

Thus, the ratio across this voltage divider at 19.4 kc and at 10 kc varies by only 2%.

Figures 3.20 through 3.39 are photographic reproductions of the signals recorded on tape during the test series. Although not of sufficient quality to allow amplitude and phase calculations, these data show characteristics of the signal as regards initial polarities, gross distortions, time duration, etc.

In addition to amplitude calculations, the film records allow an estimate of phase distortion in the underwater signal.

The effective, equivalent depth of the electrical center of the antenna is required before an attempt is made to compare attenuation versus depth.

First. The phase shift between the NPM signal into the loop and into the whip was measured, with the loop at the surface. This delay (whip to loop) was 1.66 μsec corresponding to the cable length and velocity of propagation plus loop phase shift, which was not 90° as is the case for an above-water or smaller antenna.

Second. The NPM phase shift was noted as the loop was lowered. Correlation between the measured spacing from the surface to the top of the loop is poor due primarily to wave motion and also due to the expected difficulty in predicting the electrical center of the underwater loop, since the maximum dimension of the loop is 1.414 fathoms.

Summarizing the data for two examples, Truckee and Swanee:

	Depth to Top of Loop	NPM Effective Depth	Bomb Signal Effective Depth
TRUCKEE	2 fathoms+rigging	7.34 meters	7.834 meters
SWANEE	2 fathoms+rigging ± 3- to 6-ft swells		5.3 meters (11-kc component) 5.36 meters (9.2-kc component)

Using these same examples, the computations were performed as follows:

TRUCKEE Depth/phase measurements

Estimated depth: 2 fathoms to top of loop plus rigging spacers

NPM phase measurements: inverted loop at depth phase lag, 35 μsec. Inherent loop fixed delay: 1.66 μsec. The actual phase delay was, therefore, 33.34 μsec.

Underwater phase velocity = 22 x 10^4 m/sec

= 0.22 m/μsec

Effective delay depth = 7.34 meters at 19.4 kc

to electrical center = 23.4 ft ≈ 3.9 fathoms

Shot Signal phase measurements:

Effective frequency: 5000 cps

Loop at depth phase lag: 80 μsec

Fixed delay: 1.66 μsec

Actual delay = 78.34 μsec

Phase velocity: 0.10 m/μsec

Effective delay depth 7.834 meters at 5 kc

SWANEE Depth/phase measurements

Estimated depth: 2 fathoms ±3- to 6-ft wave motion (14 ft wave maximum). Inverted signal due to

direction of loop.

First signal t_1 (peak(pos)loop) - f_1 (peak(neg)whip)=

33.6 minus 1.66 μsec = 32.0 μsec

Third signal t_3 - f_3 = 38.5 minus 1.66 μsec =

36.84 μsec

Effective frequency cross-over time

1 to 2-46.8 μsec = 11 kc

2 to 3-53.7 μsec = 9.2 kc

Phase velocity = 0.166 m/μsec at 11 kc

= 0.150 m/μsec at 9.2 kc

v x t = effective depth

(at 11 kc): 0.166 x 32 = 5.3 meters (17 feet)

(at 9.2 kc): 0.150 x 36.8 = 5.52 meters

TABLE 3.1 SUMMARY OF RECORDED EM PULSE DATA

On the tape records, the upper and lower traces are misalined due to the tape recorder. If data was recorded, the figure number of the reproduced signal is listed. If data was not recorded, NR is listed.

Due to the triggering level differences between the two ship records, a direct corresponding time comparison is not evident from these records by a casual visual inspection. Also, the apparent high-frequency peaking due to the 1,000-foot wire is evident in some USS INFLICT records.

Shot Name	Station			
	USS INFLICT		USS LOYALTY	
	Film	Tape	Film	Tape
Aztec	No data recorded			
Adobe	3.2	3.20	NR	3.20
Arkansas	NR	3.21	NR	NR
Questa	NR	3.22	NR	NR
Frigate Bird	3.3	3.23	NR	3.23
Yukon	3.4	3.24	NR	3.24
Mesilla	3.5	3.25	3.5	NR
Muskegon	3.6	NR	3.6	NR
Sword Fish	Underwater shot, no signal			
Encino	NR	NR	NR	3.25
Swanee	3.7	3.26	3.7	3.26
Chetco	3.8	3.27	3.8	3.27
Tanana	High level noise interference, no signal			
Nambe	3.9	NR	3.9	3.28
Blue Gill	Shot failed			
Alma	3.10	3.29	3.10	3.29
Truckee	NR	3.30	NR	3.30
Yeso	3.11	3.31	3.11	3.31
Harlem	3.12	3.32	3.12	3.32
Rinconada	3.13	3.33	3.13	3.33
Dulce	3.14	3.34	3.14	3.34
Star Fish	Shot failed			
Petit	3.15	3.35	3.15	3.35
Otowi	3.16	3.36	3.16	3.36
Bighorn	3.17	3.37	3.17	3.37
Bluestone	3.18	3.38	3.18	3.38
Star Fish Prime	Signal saturated equipment			
Sunset	NR	NR	NR	NR
Pamlico	3.19	3.39	3.19	3.39

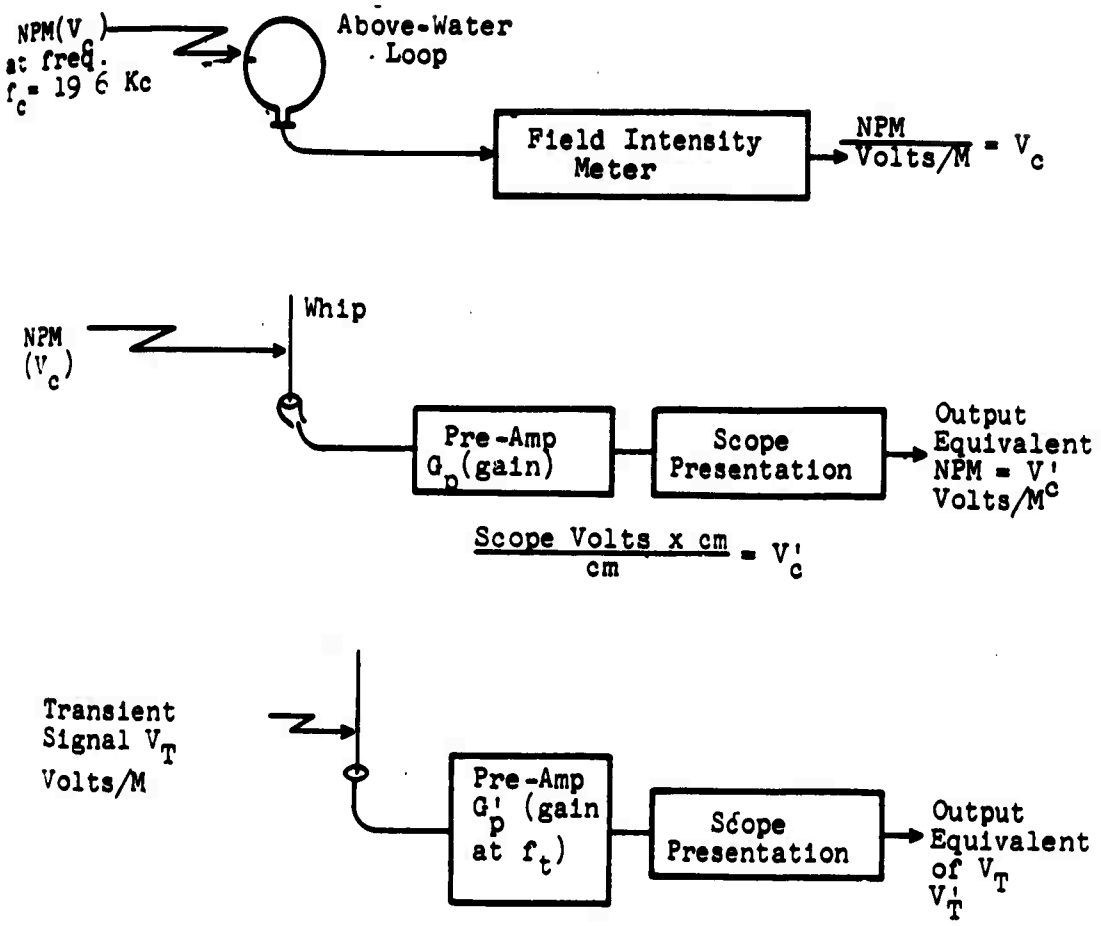

Freq. Gain Correction* $\left(\frac{G'_p}{G_p}\right)$ x $\frac{\text{Scope Volts}}{\text{cm}}$ x cm = V''_T

then $\frac{V''_T}{V'_c}$ x V_c = V_T Volts/Meter of the Transient Signal

*See Figure 2.5. This illustrates that the preamplifier was sufficiently flat so that $G'_p/G_p \approx 1.2$.

Figure 3.1 Schematic representation of calibration consideration (above water).

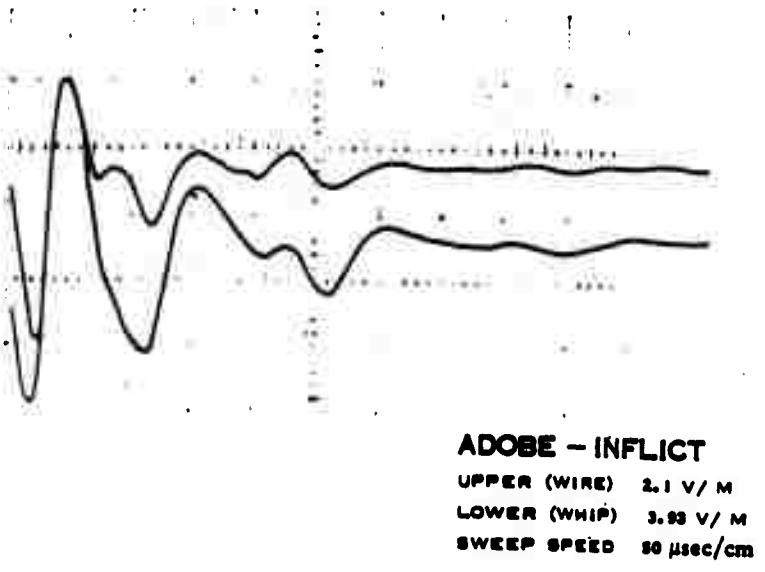

Figure 3.2 Experimental signal, film, Shot Adobe.

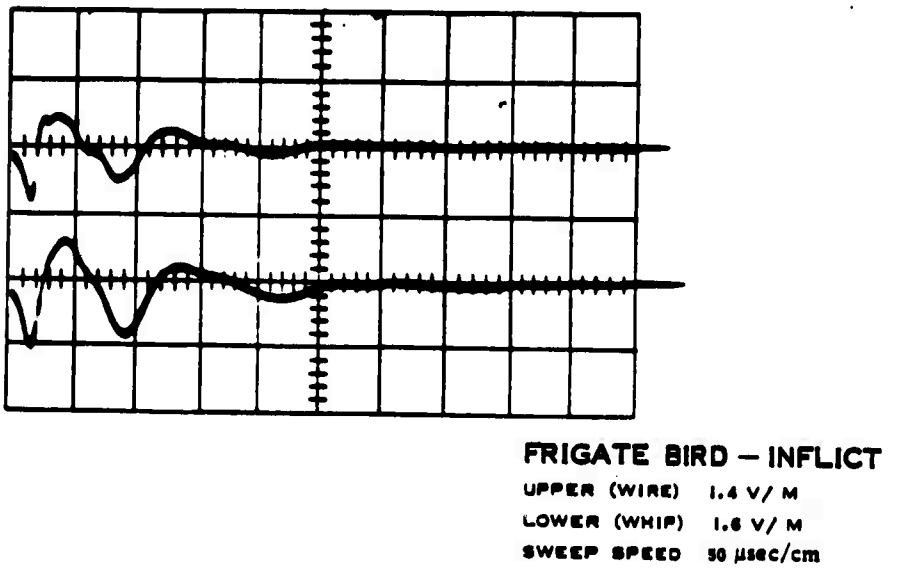

Figure 3.3 Experimental signal, film, Shot Frigate Bird.

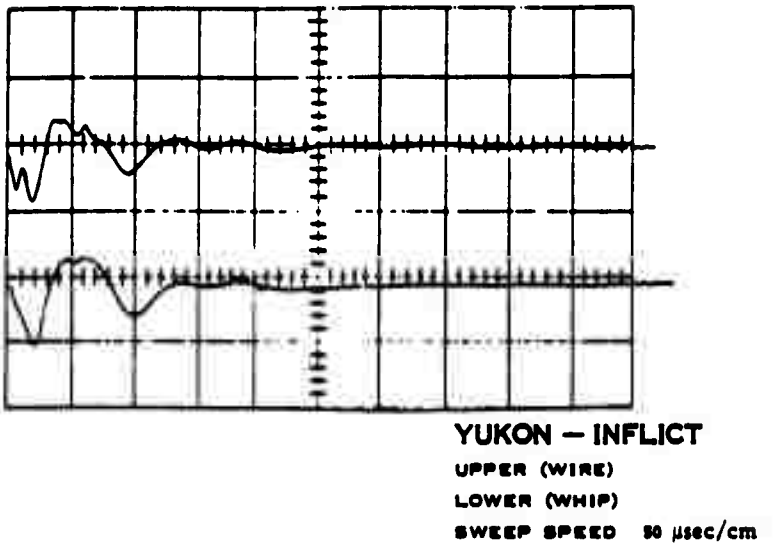

Figure 3.4 Experimental signal, film, Shot Yukon.

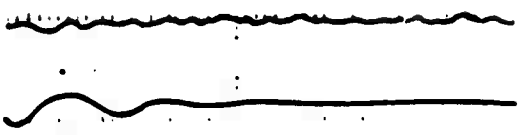

MESILLA — LOYALTY
UPPER (LOOP)
LOWER (WHIP)
SWEEP SPEED 50 μsec/cm

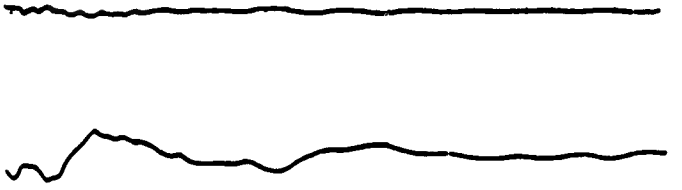

MESILLA — INFLICT
UPPER (WIRE)
LOWER (WHIP)
SWEEP SPEED 50 μsec/cm

Figure 3.5 Experimental signal, film, Shot Mesilla.

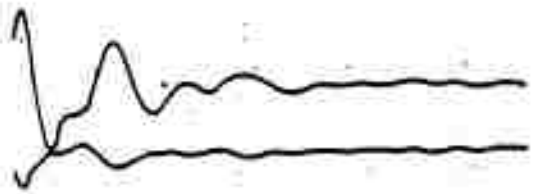

MUSKEGON — LOYALTY
UPPER (LOOP)
LOWER (WHIP)
SWEEP SPEED 50 μsec/cm

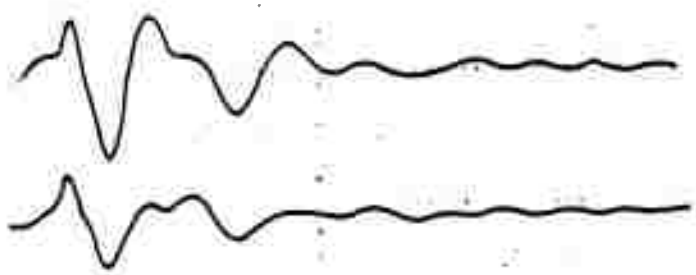

MUSKEGON — INFLICT
UPPER 2.87 V/ M (SMALL LOOP 8–10 FEET DEEP)
LOWER 1.26 V/ M (WHIP)
SWEEP SPEED 50 μsec/cm

Figure 3.6 Experimental signal, film, Shot Muskegon.

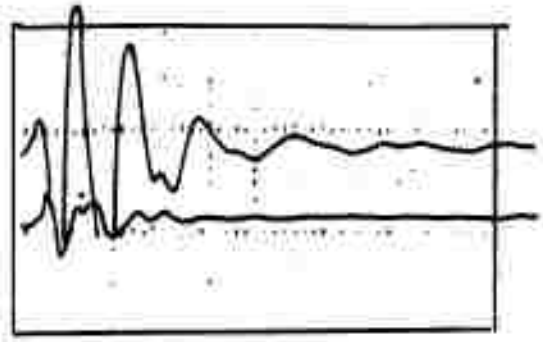

SWANEE — LOYALTY
UPPER (LOOP) 4.25 V/ M
(12 FEET DEEP)
LOWER (WHIP) 1.7 V/ M
SWEEP SPEED 100 μsec/cm

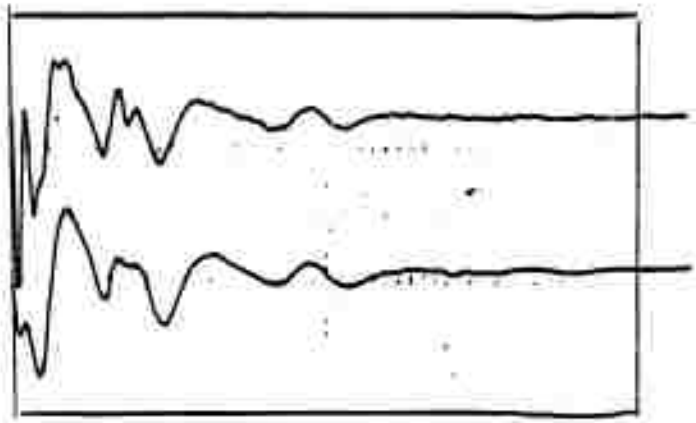

SWANEE — INFLICT
UPPER (WIRE) 2.2 V/ M
LOWER (WHIP) 1.5 V/ M
SWEEP SPEED 100 μsec/cm

Figure 3.7 Experimental signal, film, Shot Swanee.

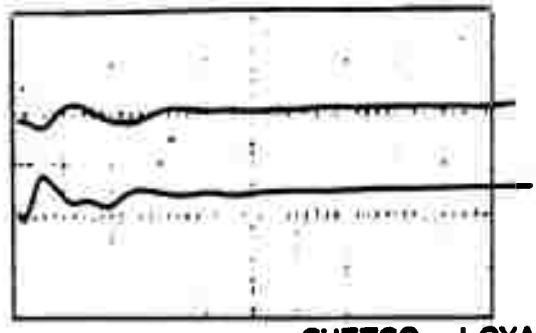

CHETCO — LOYALTY
UPPER (LOOP)
LOWER (WHIP)
SWEEP SPEED 50 μsec/cm

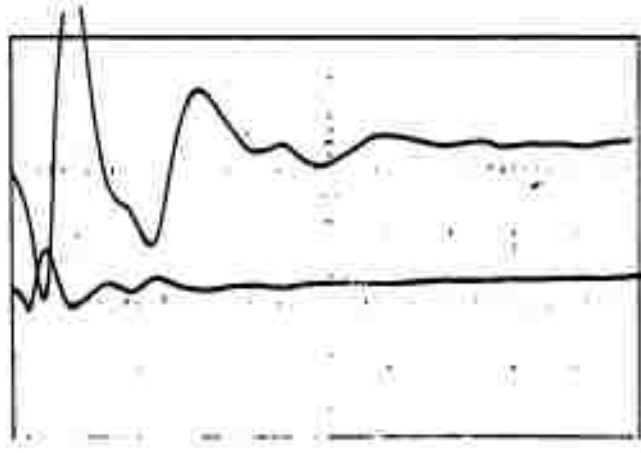

CHETCO — INFLICT
UPPER (LOOP) .75 V/ M
(23 TURN LOOP - 12 FT. DEPTH)
LOWER (WHIP) .8 V/ M
SWEEP SPEED 50 μsec/cm

Figure 3.8 Experimental signal, film, Shot Chetco.

NAMBE — LOYALTY
UPPER (LOOP)
LOWER (WHIP)
SWEEP SPEED 50 μsec/cm

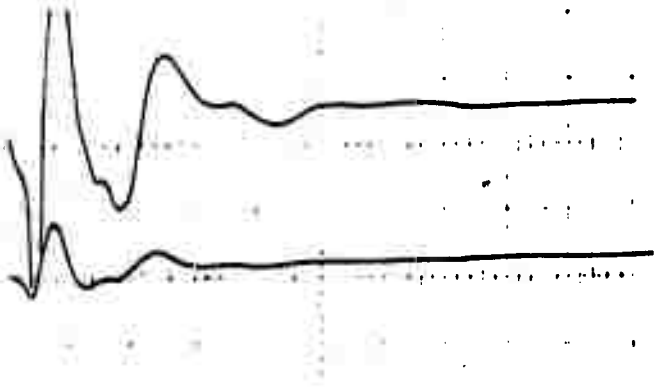

NAMBE — INFLICT
UPPER (WIRE)
LOWER (WHIP)
SWEEP SPEED 50 μsec/cm

Figure 3.9 Experimental signal, film, Shot Nambe.

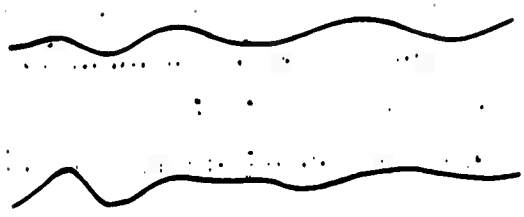

ALMA – LOYALTY
UPPER (LOOP) .7 V/ M
(23 TURN LOOP 8 FT. DEEP)
LOWER (WHIP)
SWEEP SPEED 50 μsec/cm

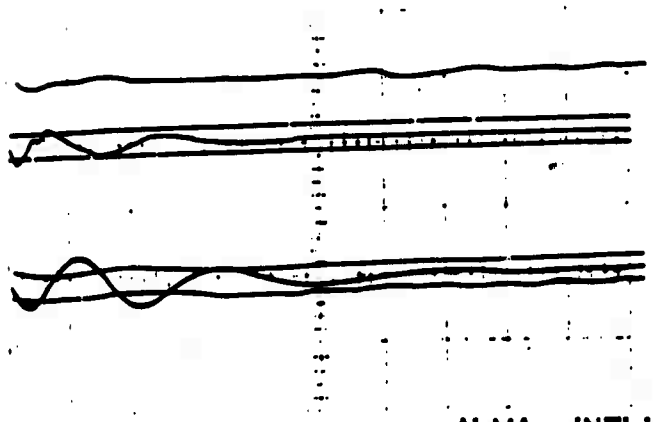

ALMA – INFLICT
UPPER (WIRE)
LOWER (WHIP)
SWEEP SPEED 50 μsec/cm

Figure 3.10 Experimental signal, film, Shot Alma.

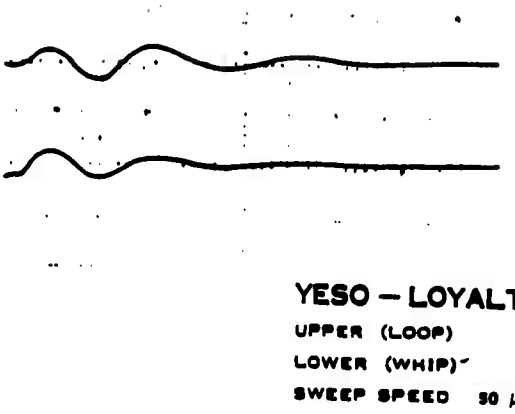

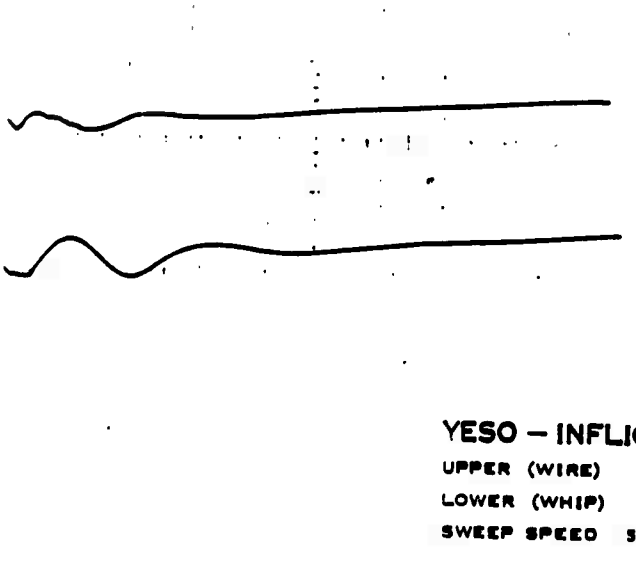

Figure 3.11 Experimental signal, film, Shot Yeso.

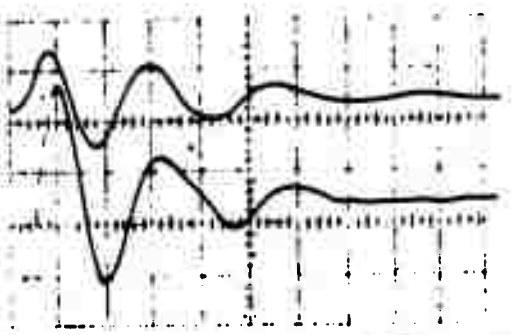

HARLEM — LOYALTY
UPPER (LOOP) 3.4 V/ M
(13 TURN LOOP 8–10 FT. DEPTH)
LOWER (WHIP) 2.2 V/ M
SWEEP SPEED 50 μsec/cm

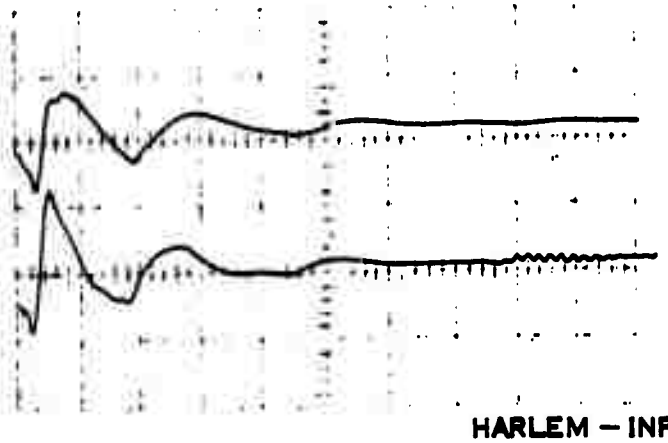

HARLEM — INFLICT
UPPER (WIRE) 1.62 V/ M
LOWER (WHIP) 2.83 V/ M
SWEEP SPEED 50 μsec/cm

Figure 3.12 Experimental signal, film, Shot Harlem.

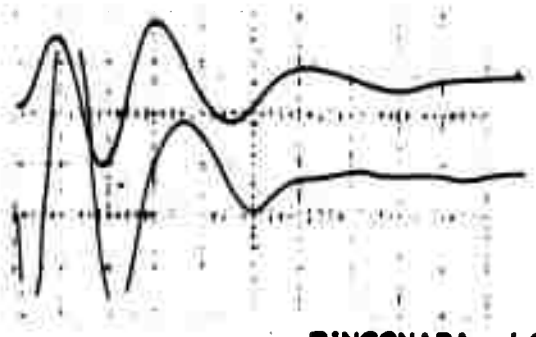

RINCONADA — LOYALTY
UPPER (LOOP) 3.2 V/ M
(23 TURNS 8 FT. DEPTH)
LOWER (WHIP) .8V/ M
SWEEP SPEED 50 μsec/cm

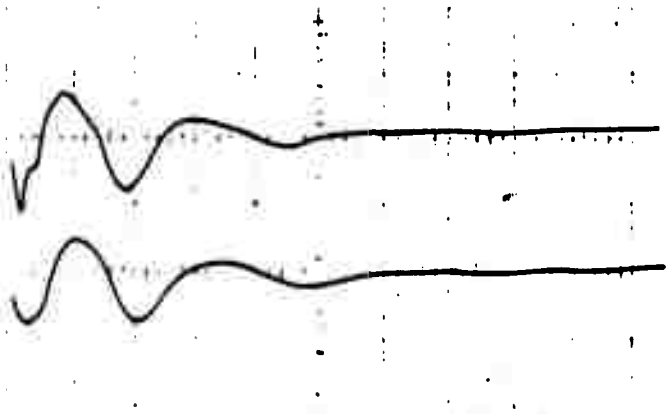

RINCONADA — INFLICT
UPPER (WIRE) 1.35 V/ M
LOWER (WHIP) .92 V/ M
SWEEP SPEED 50 μsec/cm

Figure 3.13 Experimental signal, film, Shot Rinconada.

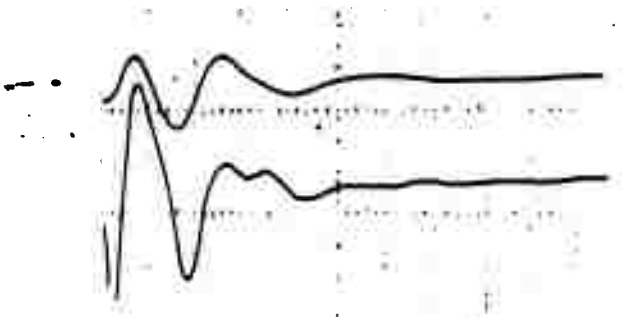

DULCE – LOYALTY
UPPER (LOOP) 1.33 V/ M
(23 TURN LOOP 2 FATHOM DEPTH)
LOWER (WHIP) .32 V/ M
SWEEP SPEED 50 μsec/cm

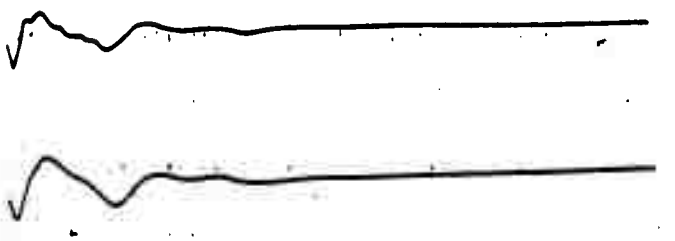

DULCE – INFLICT
UPPER (WIRE) .58 V/ M
LOWER (WHIP)
SWEEP SPEED 50 μsec/cm

Figure 3.14 Experimental signal, film, Shot Dulce.

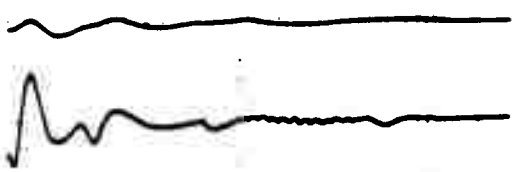

PETIT — LOYALTY
UPPER (LOOP)
LOWER (WHIP)
SWEEP SPEED 50 μsec/cm

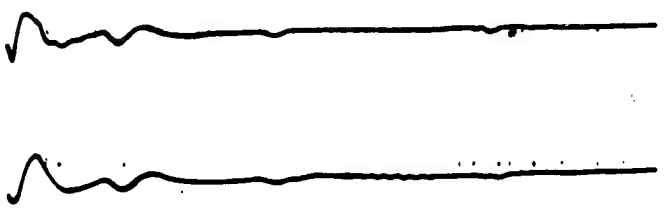

PETIT — INFLICT
UPPER (WIRE)
LOWER (WHIP)
SWEEP SPEED 50 μsec/cm

Figure 3.15 Experimental signal, film, Shot Petit.

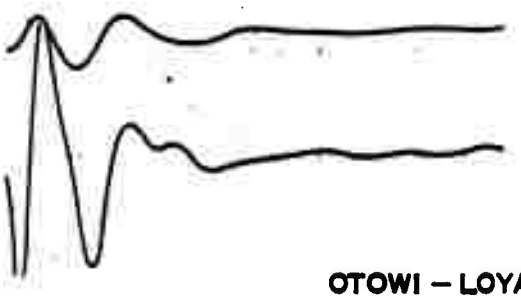

OTOWI – LOYALTY

UPPER (LOOP) .42 V/M

(23 TURN LOOP 8–10 FT. DEEP)

LOWER (WHIP) .37 V/ M

SWEEP SPEED 50 μsec/cm

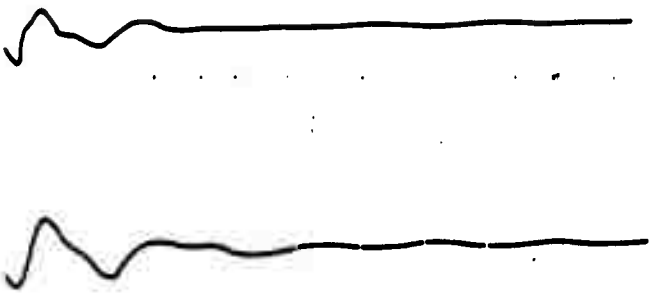

OTOWI – INFLICT

UPPER (WIRE) .46 V/ M

LOWER (WHIP) .25 V/ M

SWEEP SPEED 50 μsec/cm

Figure 3.16 Experimental signal, film, Shot Otowi.

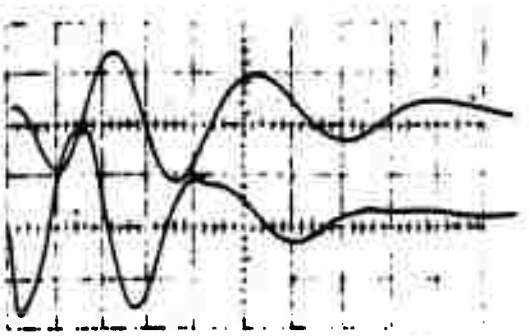

BIGHORN — LOYALTY
UPPER (LOOP) 1.95 V/ M
(23 TURN LOOP 8–10 FT. DEEP)
LOWER (WHIP) 1.4 V/ M
SWEEP SPEED 50 μsec/cm

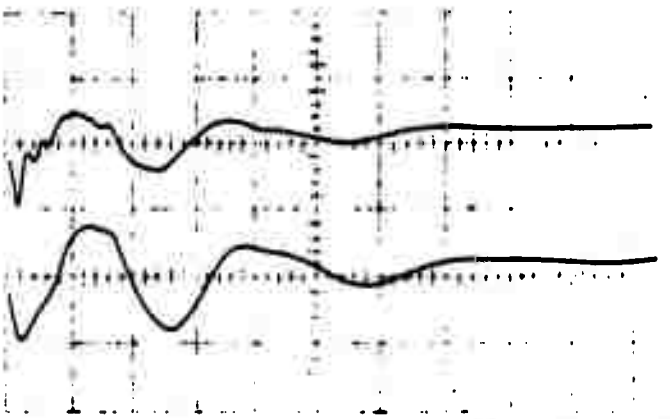

BIGHORN — INFLICT
UPPER (WIRE) 2.26 V/ M
LOWER (WHIP) 1.56 V/ M
SWEEP SPEED 50 μsec/cm

Figure 3.17 Experimental signal, film, Shot Bighorn.

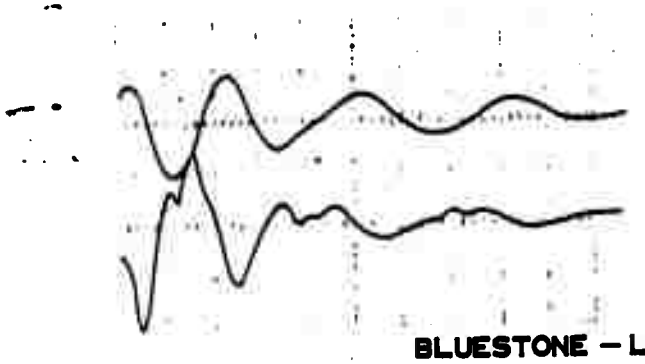

BLUESTONE — LOYALTY
UPPER (LOOP) 2.01 V/ M
(23 TURN LOOP 8-12 FT. DEPTH)
SWEEP SPEED 50 μsec/cm

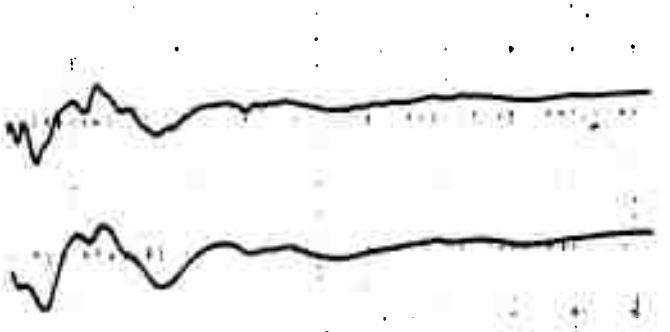

BLUESTONE — INFLICT
UPPER (WIRE) .99 V/ M
LOWER (WHIP) .62 V/ M
SWEEP SPEED 50 μsec/cm

Figure 3.18 Experimental signal, film, Shot Bluestone.

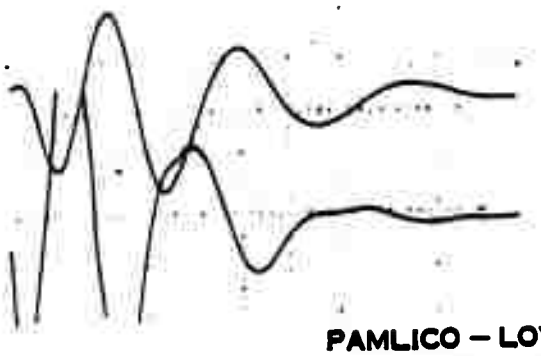

PAMLICO – LOYALTY
UPPER (LOOP) .63 V/ M
(23 TURN LOOP. 10–12 FT. DEPTH)
LOWER (WHIP) .91 V/ M
SWEEP SPEED 50 μsec/cm

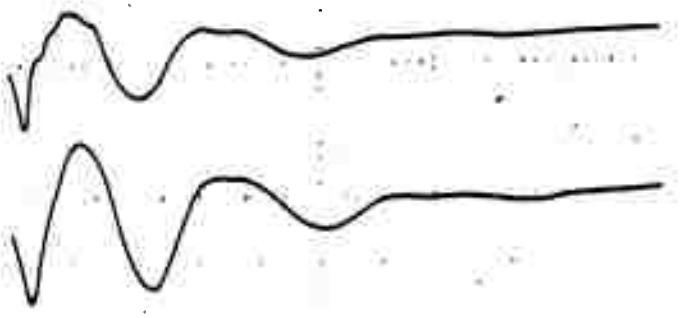

PAMLICO – INFLICT
UPPER (WIRE) 1.23 V/ M
LOWER (WHIP) 1.2 V/ M
SWEEP SPEED 50 μsec/cm

Figure 3.19 Experimental signal, film, Shot Pamlico.

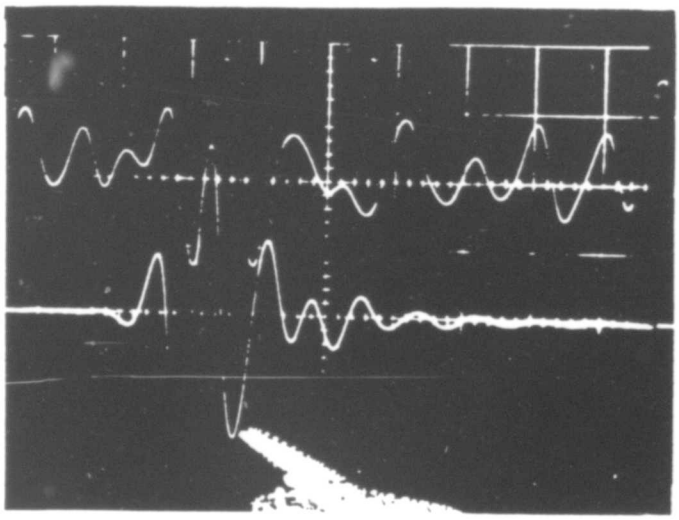

ADOBE: USS LOYALTY
Upper-loop, lower-whip
Sweep speed, 0.1 msec/cm

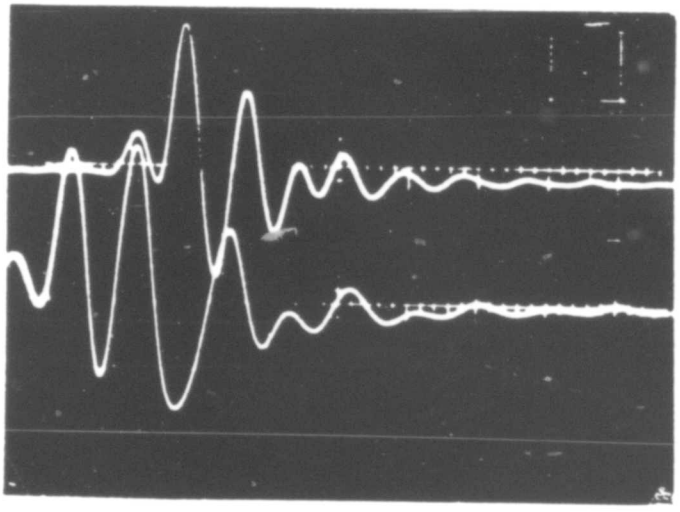

ADOBE: USS INFLICT
Upper-wire, lower-whip
Sweep speed, 0.1 msec/cm

Figure 3.20 Experimental signal, tape, Shot Adobe.

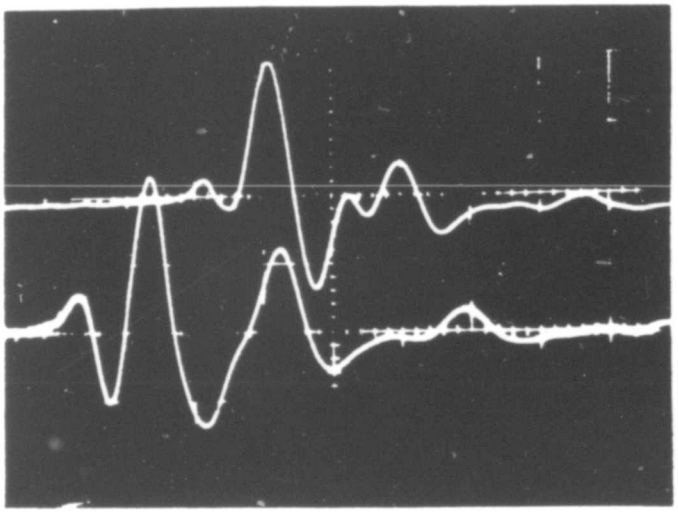

ARKANSAS: USS INFLICT
Upper-wire, lower-whip
Sweep speed, 0.1 msec/cm

Figure 3.21 Experimental signal, tape, Shot Arkansas.

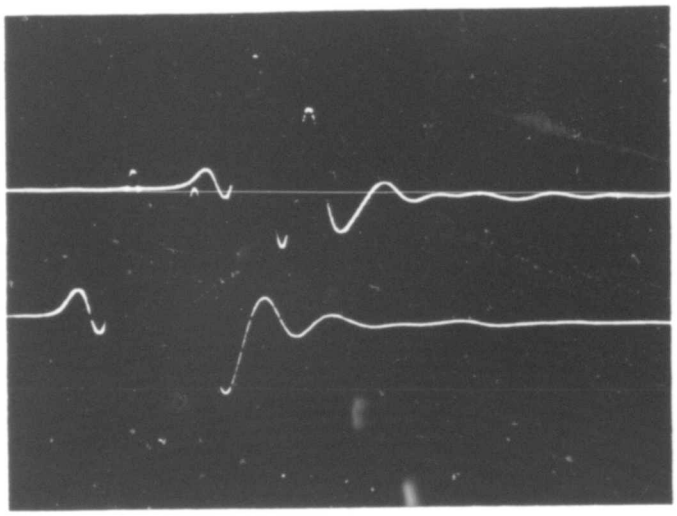

QUESTA: USS INFLICT
Upper-wire, lower-whip
Sweep speed, 0.1 msec/cm

Figure 3.22 Experimental signal, tape, Shot Questa.

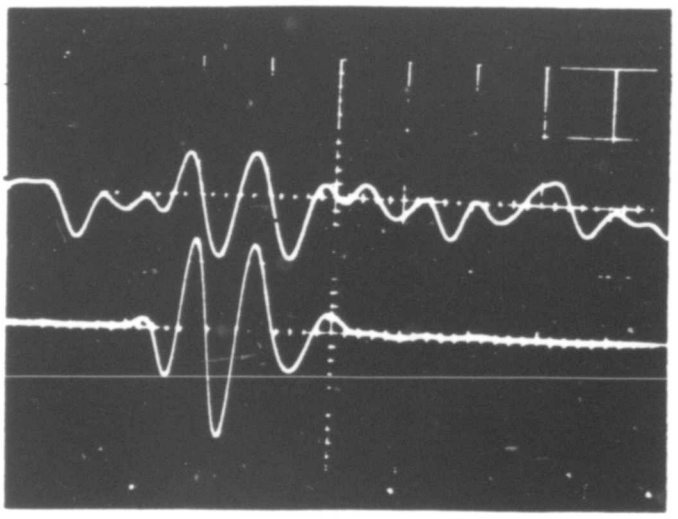

FRIGATE BIRD: USS LOYALTY
Upper-loop, lower-whip
Sweep speed, 0.1 msec/cm

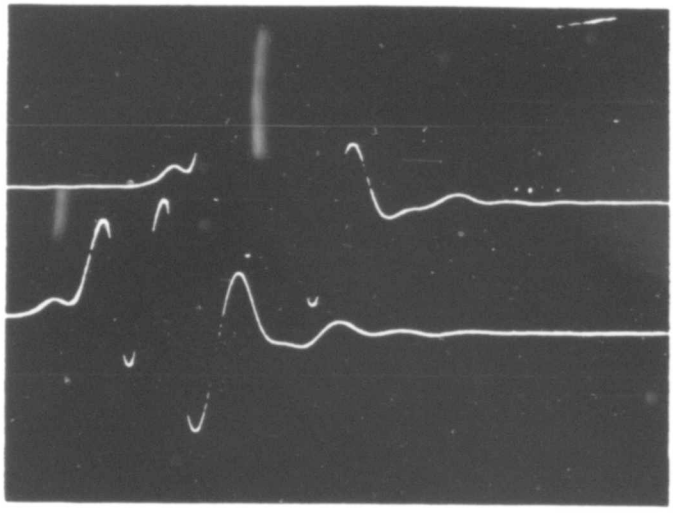

FRIGATE BIRD: USS INFLICT
Upper-wire, lower-whip
Sweep speed, 0.1 msec/cm

Figure 3.23 Experimental signal, tape, Shot Frigate Bird.

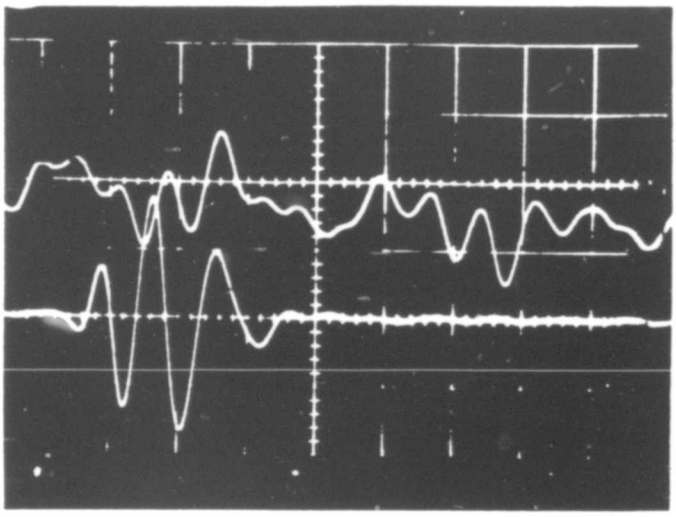

YUKON: USS LOYALTY
Upper-loop, lower-whip
Sweep speed, 0.1 msec/cm

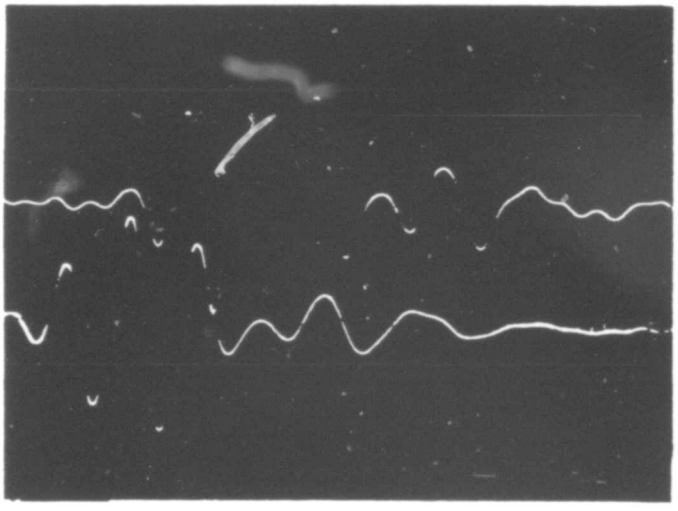

YUKON: USS INFLICT
Upper-wire, lower-whip
Sweep speed, 0.1 msec/cm

Figure 3.24 Experimental signal, tape, Shot Yukon.

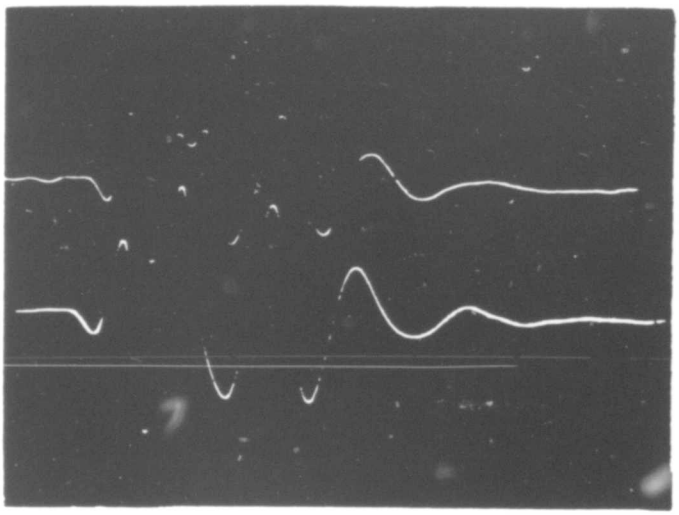

MESILLA: USS INFLICT
Upper-wire, lower-whip
Sweep speed, 0.1 msec/cm

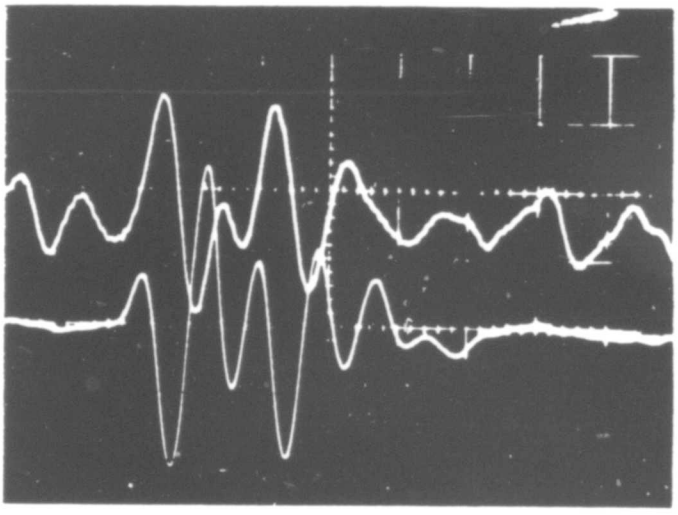

ENCINO: USS LOYALTY
Upper-loop, lower-whip
Sweep speed, 0.1 msec/cm

Figure 3.25 Experimental signals, tape, Shots Mesilla and Encino.

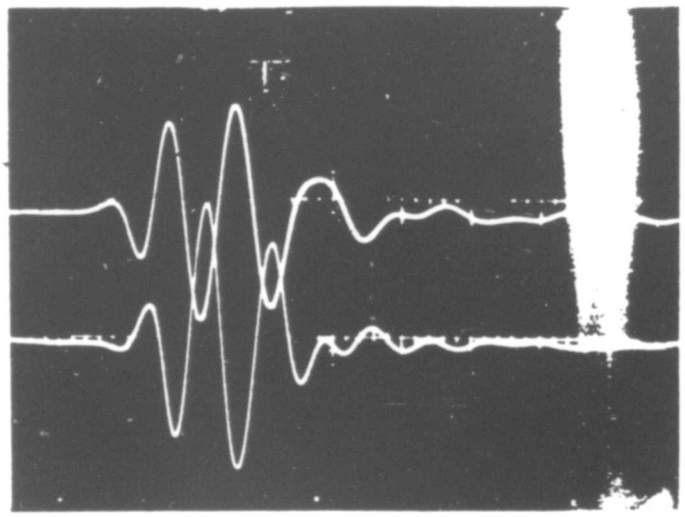

SWANEE: USS LOYALTY
Upper-loop, lower-whip
Sweep speed, 0.1 msec/cm

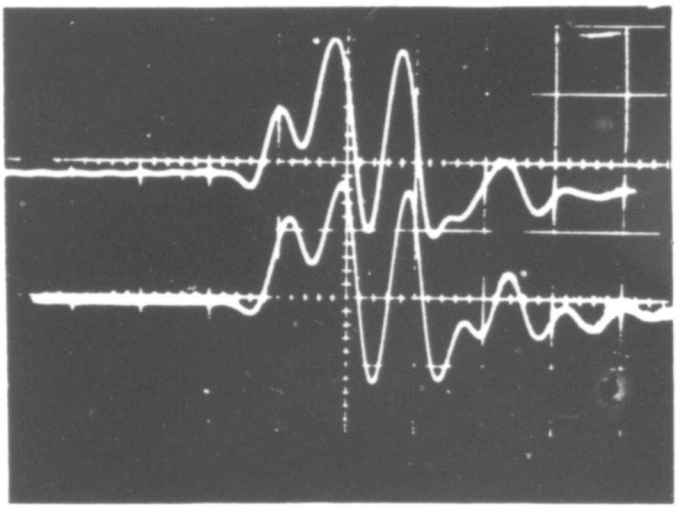

SWANEE: USS INFLICT
Upper-wire, lower-whip
Sweep speed, 0.1 msec/cm

Figure 3.26 Experimental signal, tape, Shot Swanee.

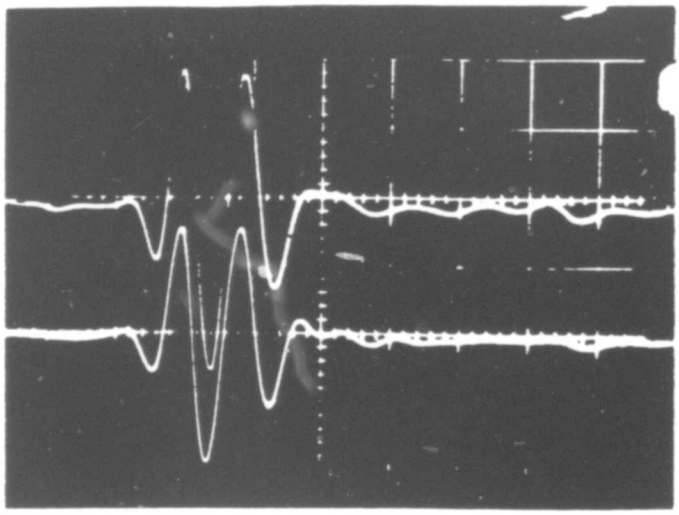

CHETCO: USS LOYALTY
Upper-loop, lower-whip
Sweep speed, 0.1 msec/cm

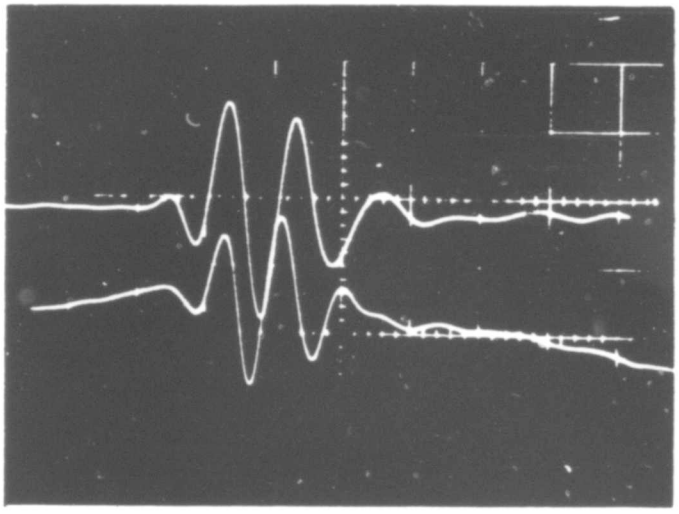

CHETCO: USS INFLICT
Upper-loop, lower-whip
Sweep speed, 0.1 msec/cm

Figure 3.27 Experimental signal, tape, Shot Chetco.

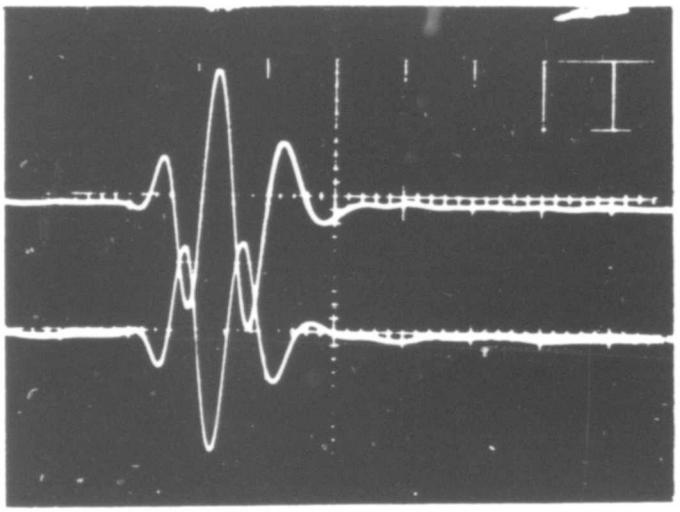

NAMBE: USS LOYALTY
Upper-loop, lower-whip
Sweep speed, 0.1 msec/cm

Figure 3.28 Experimental signal, tape, Shot Nambe.

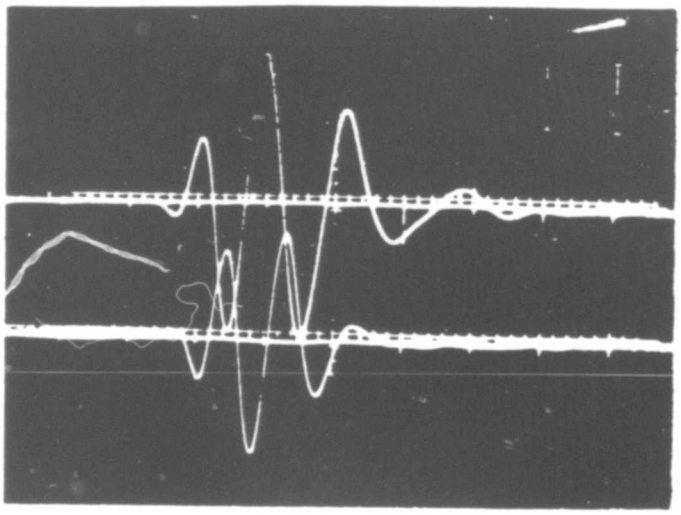

ALMA: USS LOYALTY
Upper-loop, lower-whip
Sweep speed, 0.1 msec/cm

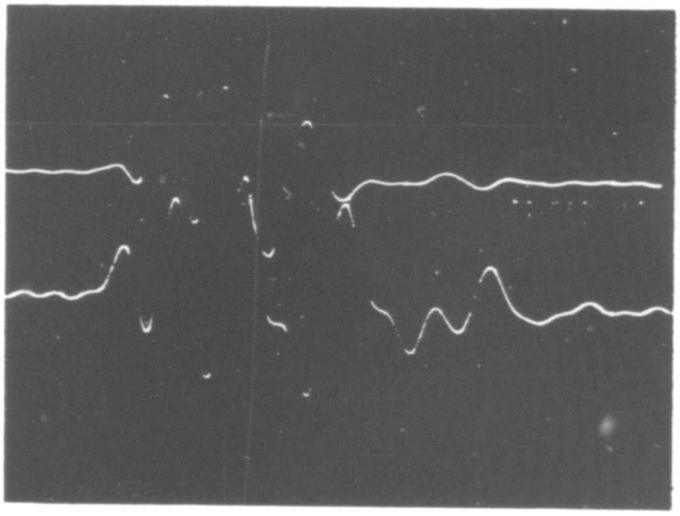

ALMA: USS INFLICT
Upper-wire, lower-whip
Sweep speed, 0.1 msec/cm

Figure 3.29 Experimental signal, tape, Shot Alma.

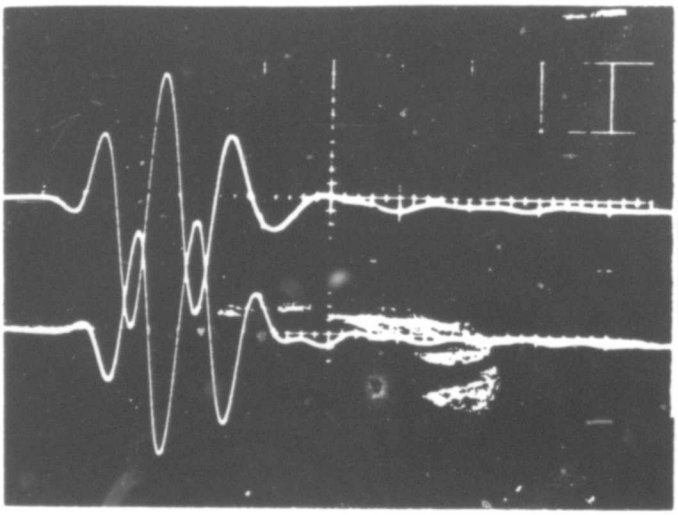

TRUCKEE: USS LOYALTY
Upper-loop, lower-whip
Sweep speed, 0.1 msec/cm

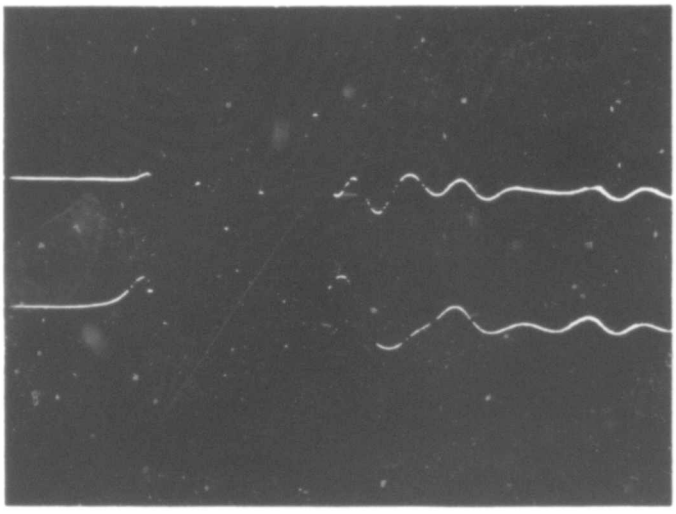

TRUCKEE: USS INFLICT
Upper-wire, lower-whip
Sweep speed, 0.1 msec/cm

Figure 3.30 Experimental signal, tape, Shot Truckee.

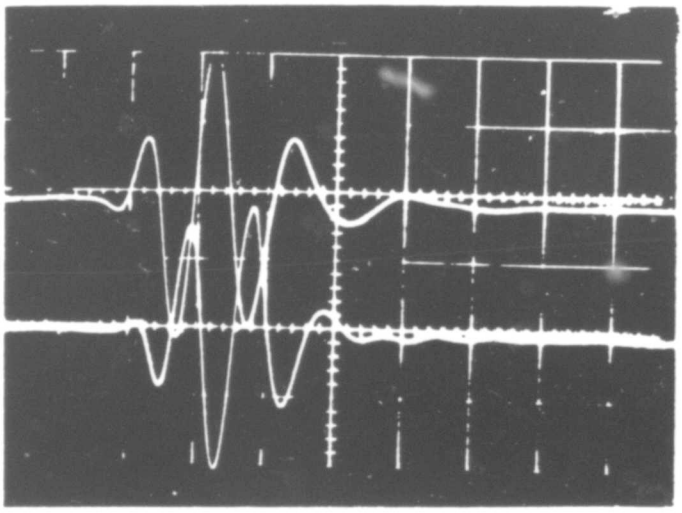

YESO: USS LOYALTY
Upper-loop, lower-whip
Sweep speed, 0.1 msec/cm

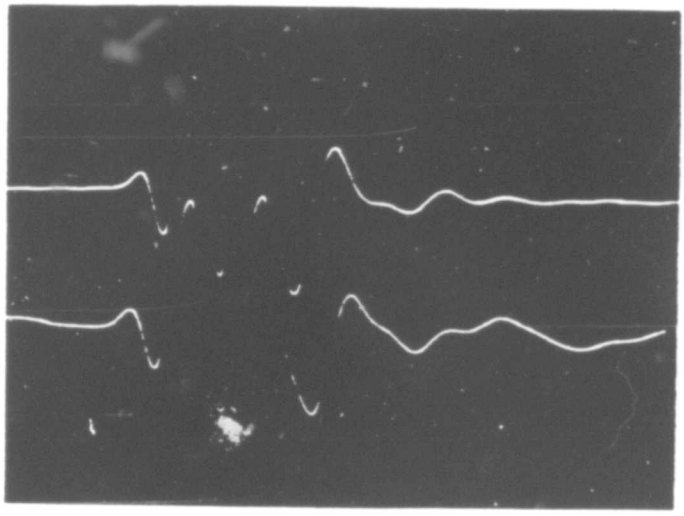

YESO: USS INFLICT
Upper-wire, lower-whip

Figure 3.31 Experimental signal, tape, Shot Yeso.

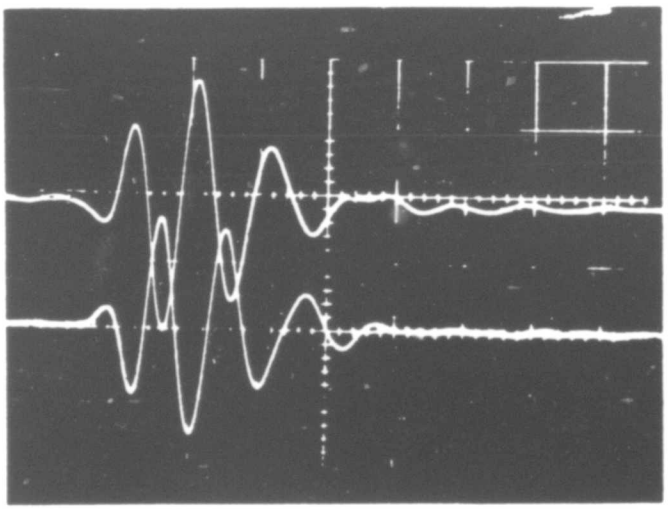

HARLEM: USS LOYALTY
Upper-loop, lower-whip
Sweep speed, 0.1 msec/cm

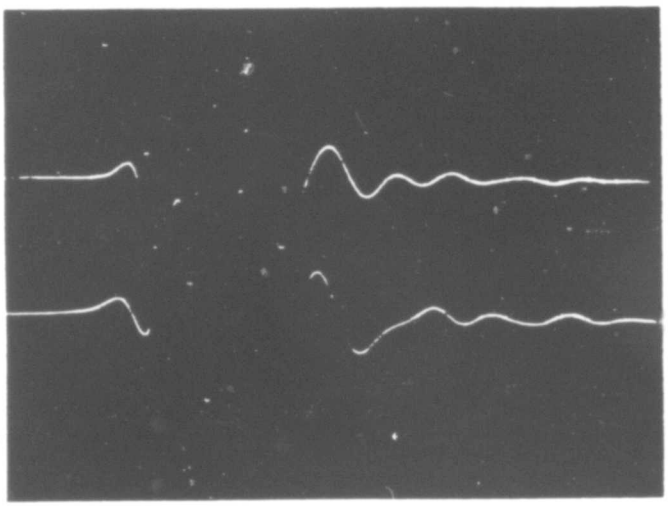

HARLEM: USS INFLICT
Upper-wire, lower-whip
Sweep speed, 0.1 msec/cm

Figure 3.32 Experimental signal, tape, Shot Harlem.

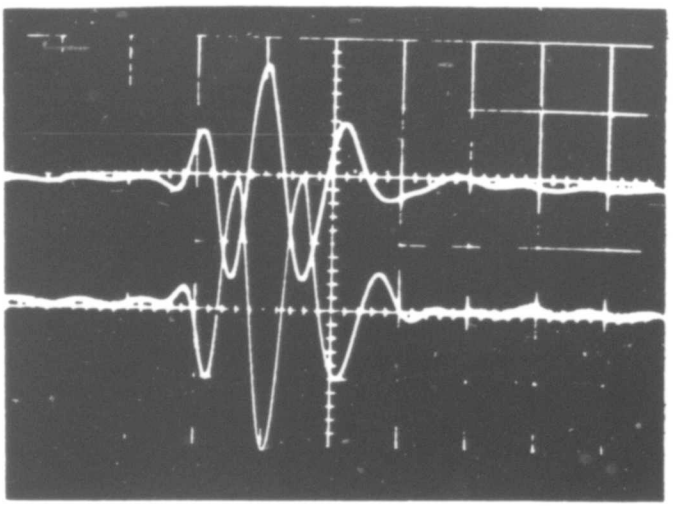

RINCONADA: USS LOYALTY
Upper-loop; lower-whip
Sweep speed, 0.1 msec/cm

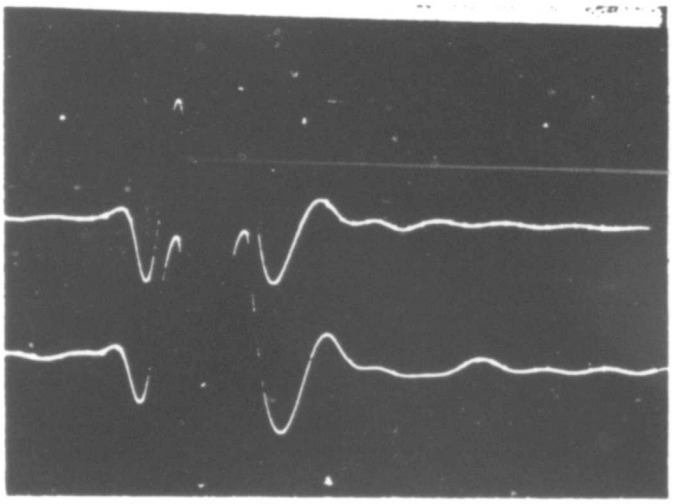

RINCONADA: USS INFLICT
Upper-wire, lower-whip
Sweep speed, 0.1 msec/cm

Figure 3.33 Experimental signal, tape, Shot Rinconada.

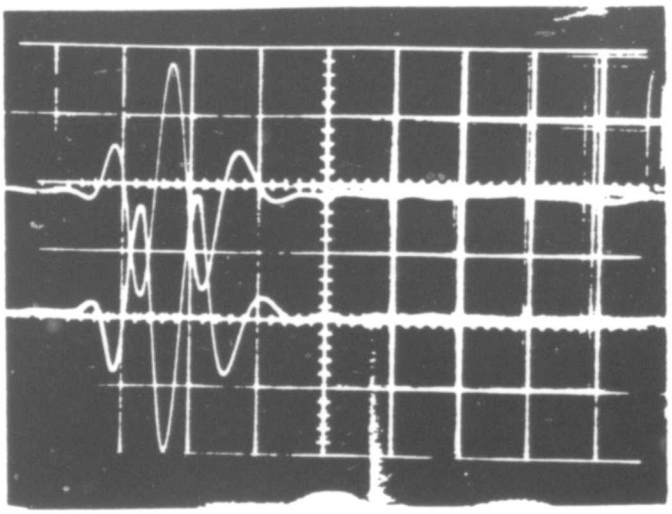

DULCE: USS LOYALTY
Upper-loop, lower-whip
Sweep speed, 0.1 msec/cm

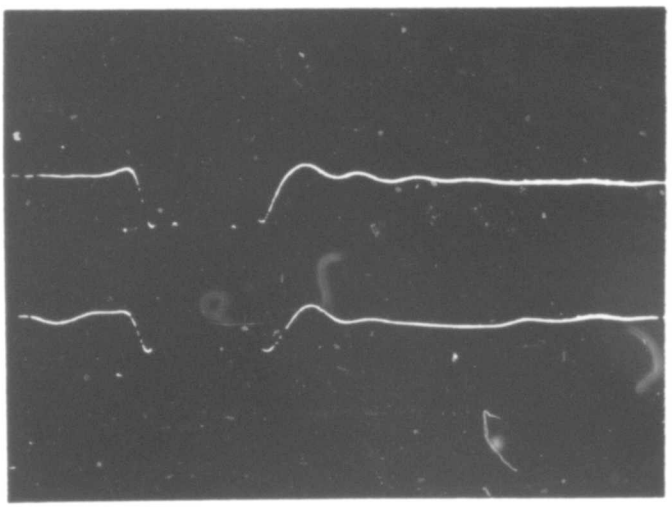

DULCE: USS INFLICT
Upper-wire, lower-whip
Sweep speed, 0.1 msec/cm

Figure 3.34 Experimental signal, tape, Shot Dulce.

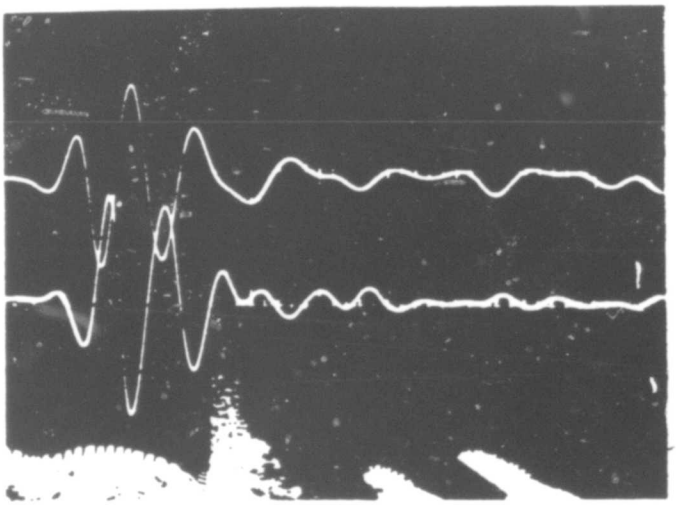

PETIT: USS LOYALTY
Upper-loop, lower-whip
Sweep speed, 0.1 msec/cm

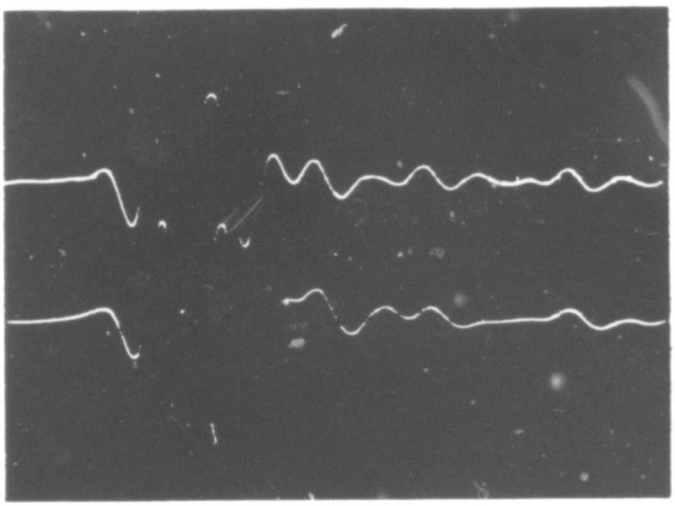

PETIT: USS INFLICT
Upper-wire, lower-whip
Sweep speed, 0.1 msec/cm

Figure 3.35 Experimental signal, tape, Shot Petit.

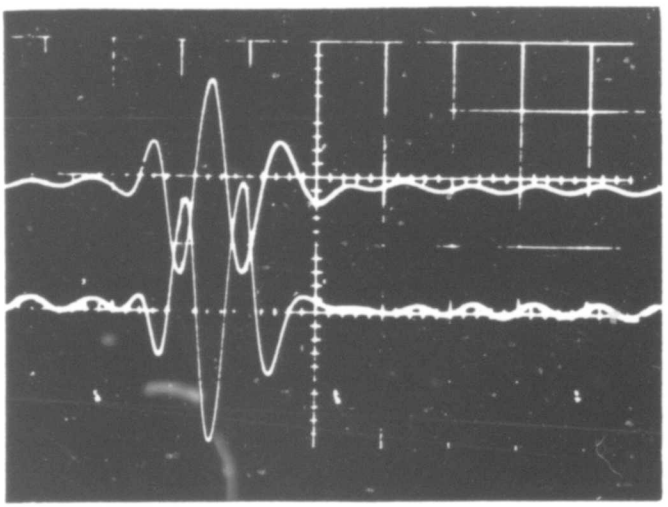

OTOWI: USS LOYALTY
Upper-loop, lower-whip
Sweep speed, 0.1 msec/cm

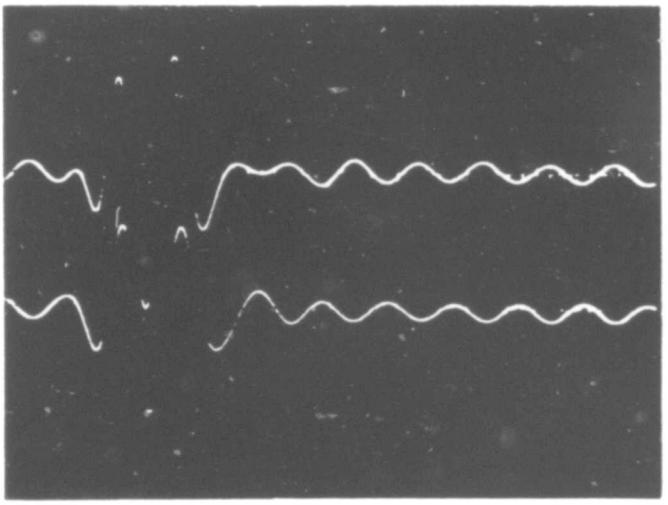

OTOWI: USS INFLICT
Upper-wire, lower-whip
Sweep speed, 0.1 msec/cm

Figure 3.36 Experimental signal, tape, Shot Otowi.

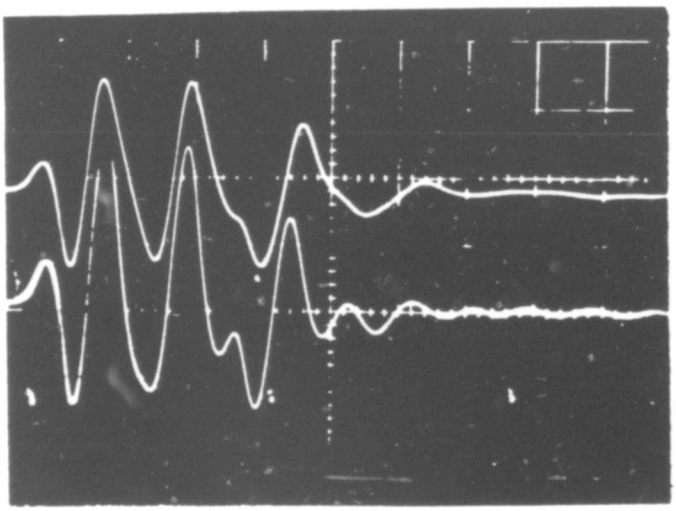

BIGHORN: USS LOYALTY
Upper-loop, lower-whip
Sweep speed, 0.1 msec/cm

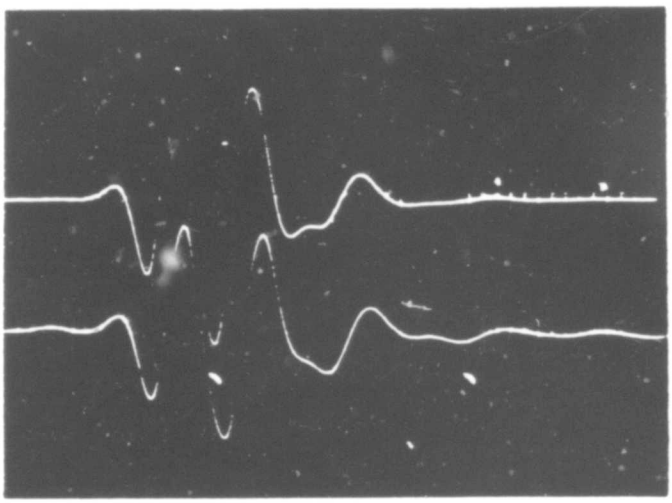

BIGHORN: USS INFLICT
Upper-wire, lower-whip
Sweep speed, 0.1 msec/cm

Figure 3.37 Experimental signal, tape, Shot Bighorn.

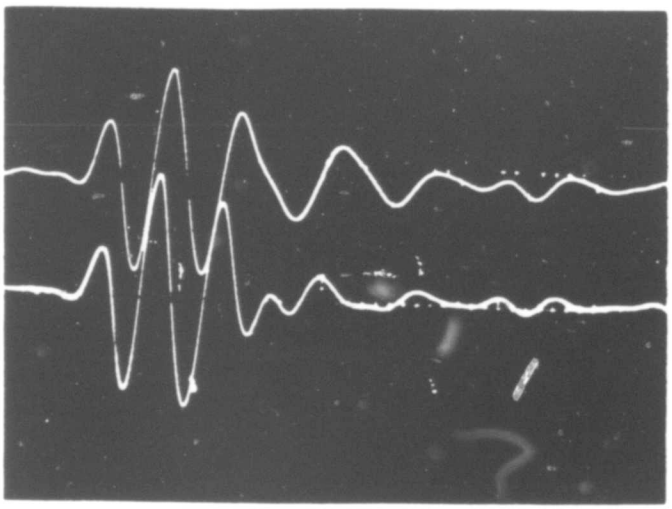

BLUESTONE: USS LOYALTY
Upper-loop, lower-whip
Sweep speed, 0.1 msec/cm

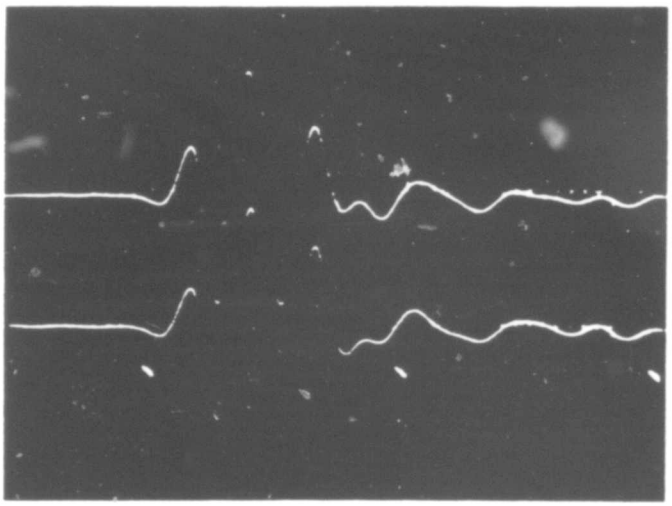

BLUESTONE: USS INFLICT
Upper-wire, lower-whip
Sweep speed, 0.1 msec/cm

Figure 3.38 Experimental signal, tape, Shot Bluestone.

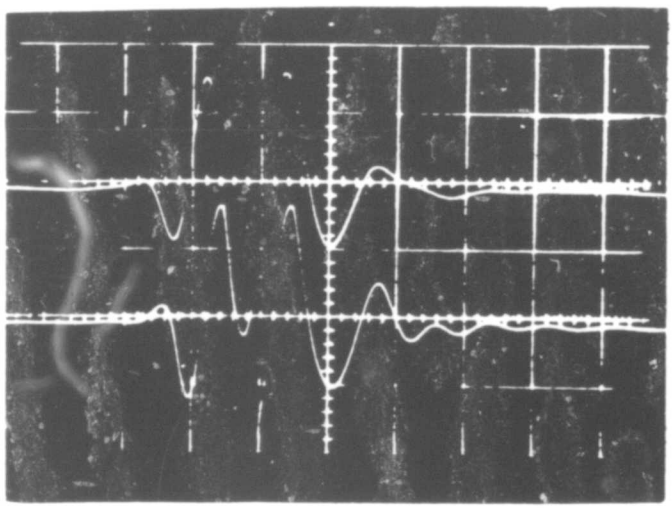

PAMLICO: USS LOYALTY
Upper-loop, lower-whip
Sweep speed, 0.1 msec/cm

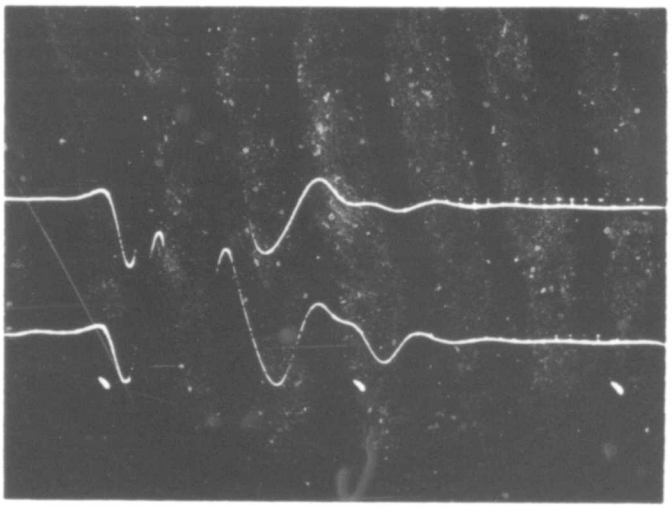

PAMLICO: USS INFLICT
Upper-wire, lower-whip
Sweep speed, 0.1 msec/cm

Figure 3.39 Experimental signal, tape, Shot Pamlico.

CHAPTER 4

CONCLUSIONS

The data accumulated on the EM pulse generated by the series of shots in this test are sufficient to confirm the feasibility of an IBDA system. The desired information on the effect of air-water phase shift and attenuation on transmission of VLF signals is readily available using the recorded data.

Equipment limitations influenced the majority of data taken; nevertheless, the objectives of the program were fulfilled. If such a measurement program were to be undertaken in the future, sufficient lead time should be made available for the preparation of higher quality equipment.

The results illustrate that a submarine can be a useful observational station for detecting not only the self-launched nuclear weapons but could also detect other nuclear bursts. This has operational significance in cases where information on nearby nuclear action would be of value to the operational submarine.

The decrease in noise level for underwater antennas is very significant and results in further optimism

regarding the depth to which underwater antennas could detect the relatively strong nuclear signals. This noise reduction was not observed on the long, floating wire antenna.

REFERENCES

1. "A Preliminary Study of A Surveillance System(U)", KN-62-790A(R), 12 January 1962, Kaman Nuclear, Secret Restricted Data.

2. "Feasibility of An Indirect Bomb Damage Assessment System for the Mark 2 Polaris Submarine(U)", KN-61-730(P), 25 April 1961, Kaman Nuclear, Secret Restricted Data.

3. "A Nuclear Surveillance System for the Polaris Submarine(U)", KN-60-7(R), 28 January 1960, Secret Restricted Data.

4. J. P. Wesley, "Theory of Electromagnetic Field From a Ground Shot:, UCRL-5177, Lawrence Radiation Laboratory, Livermore, California, July 1958, Confidential-Formerly Restricted Data.

5. R. E. Clapp, "Coherent Radiation From Nuclear Detonations(U)", Report No. 264E002, 27 July 1956, Ultrasonic Corporation, Secret Restricted Data.

6. J. A. Kemper and Herbert Reno, "HARDTACK, Phase I: Waveforms and Spectra", NBS Report 3CB107, September 1959, National Bureau of Standards, Secret Restricted Data.

7. A. G. Jean, Jr., and W. L. Taylor, "Quarterly Report On Project T/620/E-NBS for Period Ending December 30, 1955", NBS Report 3C121, Secret Restricted Data.

8. R. M. Kloepper, "Electromagnetic Measurements", WT-1223, Operation TEAPOT, Project 13.3C, 9 May 1957, Los Alamos Scientific Laboratory, Secret Restricted Data.

9. S. D. Abercrombie, "A Note on United Kingdom Electromagentic Recording System as at Present Used for Nuclear Surveillance and Possible Future Developments", Notes from Disarmament Conference.

10. W. C. Johnson, "Amateur V.L.F. Observation QST", March 1960, and private correspondence, 1961.

11. Chin-Lin Chen, "The Small Loop Antenna in a Dissipative Medium", Cruft Laboratory Technical Report 369.

Page 97 deleted